SYSTEMS, SCIENCE AND SOFTWARE

FINAL REPORT (DRAFT)

AD-A259 255

SSS-R-81-5149

CALCULATIONAL INVESTIGATION FOR MINE-CLEARANCE EXPERIMENTS

Charles E. Needham
Joseph E. Crepeau

Systems, Science and Software
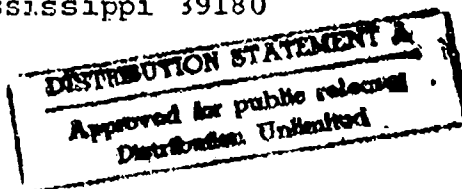P. O. Box 8243
Albuquerque, New Mexico 87198

DTIC
SELECTE
JAN 12 1993
B

31 August 1981

CONTRACT DACA39-80-C-0018

93-00697

Prepared for

Commander and Director
U.S. Army Corps of Engineers
Waterways Experiment Station
P.O. Box 631
Vicksburg, Mississippi 39180

93 1 11 087

ALBUQUERQUE OFFICE – TELEPHONE (505) 265-5895
MAIL ADDRESS: P.O. BOX 8243, ALBUQUERQUE, NM 87198

P. O. BOX 1620, LA JOLLA, CALIFORNIA 92038, TELEPHONE (714) 453-0060

PAGES _____ ARE MISSING IN ORIGINAL DOCUMENT

REPORT DOCUMENTATION PAGE		READ INSTRUCTIONS BEFORE COMPLETING FORM
1. REPORT NUMBER SSS-R-81-5149	2. GOVT ACCESSION NO.	3. RECIPIENT'S CATALOG NUMBER
4. TITLE (and Subtitle) CALCULATIONAL INVESTIGATION FOR MINE-CLEARANCE EXPERIMENTS		5. TYPE OF REPORT & PERIOD COVERED FINAL DRAFT REPORT
		6. PERFORMING ORG. REPORT NUMBER SSS-R-81-5149
7. AUTHOR(s) Charles E. Needham Joseph E. Crepeau		8. CONTRACT OR GRANT NUMBER(s) DACA39-80-C-0018
9. PERFORMING ORGANIZATION NAME AND ADDRESS Systems, Science and Software P. O. Box 8243 Albuquerque, New Mexico 87198		10. PROGRAM ELEMENT, PROJECT, TASK AREA & WORK UNIT NUMBERS
11. CONTROLLING OFFICE NAME AND ADDRESS US Army Engineer Waterways Experiment Station P.O. Box 631, Vicksburg, Miss. 39180		12. REPORT DATE 31 August 1981
		13. NUMBER OF PAGES 70
14. MONITORING AGENCY NAME & ADDRESS(If different from Controlling Office)		15. SECURITY CLASS. (of this report) UNCLASSIFIED
		15a. DECLASSIFICATION/DOWNGRADING SCHEDULE

16. DISTRIBUTION STATEMENT (of this Report)

This report was brought to the Library by
Dr. Guy Jackson, Jr., Structures Laboratory
on 21 December 1991 with the request that
it be cataloged and placed in the WES Library.
This contract report was originally desig-
nated as TR SL-82-1, but due to funding
it was never published.

17. DISTRIBUTION STATEMENT

18. SUPPLEMENTARY NOTES

19. KEY WORDS (Continue on reverse side if necessary and identify by block number)

Line-Charge Effects, Mine Clearance, Skip Zone, Airblast, Hydro-
dynamic Computer Calculations, High Explosive Experiments, Line
Charge Experiments, Line-Charge Calculations, and Charge
Configuration Improvement

20. ABSTRACT (Continue on reverse side if necessary and identify by block number)

The detonation of military line charges is being considered as a
means to clear battlefields of implanted pressure-sensitive anti-
tank mines. Such charges have an undesirable characteristic,
however, in that, for distances less than about 1 m from the line
charge, phase duration of the positive overpressure is too short
to detonate the mines. This region in which mine clearance may
not occur is called the "skip zone".

PREFACE

DTIC QUALITY INSPECTED 1

Accession For

NTIS GRA&I	☑
DTIC TAB	☐
Unannounced	☐
Justification	

By perform 5D
Distribution/

Availability Codes

| Dist | Avail and/or Special |
| A-1 | |

1

UNANNOUNCED

CONTENTS

LIST OF FIGURES (Continued)

3

LIST OF FIGURES (Continued)

CALCULATIONAL INVESTIGATION FOR MINE CLEARANCE EXPERIMENTS

PART I: INTRODUCTION

1. The Marine Corps M58 A1 and the British Giant Viper (BGV) line charges are under consideration as viable means for pressure sensitive antitank mine clearance. An important deciding factor lies in the elimination of an undesirable characteristic of the charge, referred to as the "skip zone". The skip zone is a region extending axially down the length of the charge and perpendicularly to a radius of about 1 m, in which some of the mines fail to detonate. The reason seems to lie in the charge airblast characteristics in this region. Here the overpressure waveform is defined by a high-amplitude shock with an extremely brief positive duration. This results in a lowered overpressure impulse causing mines to remain untriggered. Thus, the main objective of this calculational effort was to determine an improved charge configuration that would enhance the overpressure impulse in this region to effect reliable mine detonation.

2. The U.S. Army Engineer Waterways Experiment Station (WES) has conducted several line-charge tests in order to obtain experimental airblast data[1]. In conjunction, Systems, Science and Software (S^3) has performed various one-dimensional hydrodynamic computer calculations of detonation of the line charges. The following pages introduce the calculations and present comparisons of data from both efforts. Some possible improvements to the charge configuration to minimize skip zone effects are suggested.

PART II. LINE-CHARGE AIRBLAST CHARACTERISTICS

3. Under a previous contract with WES, S^3 made hydro-
dynamic calculations to determine the validity of the experi-
mental data and the reason for the existence of the skip zone.
The Spherical Air Puff (SAP) one-dimensional, multimaterial
hydrocode developed at the Air Force Weapons Laboratory (AFWL),
was used for the calculations[2]. SAP was run in the Lagrangian
mode using cylindrical geometry. An equation of state for
pentolite was used to calculate the hydrodynamic parameters
during the high-explosive (HE) burn. "Snapshots", logarithmi-
cally spaced in time, of pressure, density, velocity, and
temperature were taken. These snapshots enable one to follow
shocks as they propagate through space. An insight into the
causes of certain phenomena seen in experimental data is thus
gained. Points fixed in space, or stations, were also placed
at several radii of interest. Hydrodynamic variables were
monitored at each station to obtain parameter versus time data.
These data are used for direct comparison with experimental
gage records.

Shock History

4. An understanding of airblast shock formation and
propagation may be obtained by "walking through" the shock
wave history from one calculation. SAP Problem 5.0002 is a
15.12 kg/m line-charge calculation and its airblast history
will be used for this purpose.

5. Initially, in the charge region, the radial velocity
is zero and the pressure is large (by five orders of magnitude)
compared to ambient air pressure. The high pressure is due
to an initial energy density of 5.155×10^{13} ergs/kg. These
initial conditions cause large accelerations and hence material
velocities of up to 5 kmps by the time the shock front reaches

two charge radii. A rarefaction wave reaches the charge center at the time the shock front reaches three charge radii. The high-density detonation products expand and cool while the air is swept out and compressed into a thin shell surrounding the detonation products. When the shock reaches seven charge radii, the pressure in the shell of air is comparable to that inside the detonation products and the air density is ten times atmospheric. When the shock reaches twenty charge radii, the detonation products have expanded to form a cylindrical shell with a nearly evacuated center. A shock begins to form on the inner surface of the shell while the thickness of the shell increases as it grows radially.

6. The inner surface of the high-density detonation products stops expanding when the shock reaches eighty charge radii. The outer edge of the detonation products has reached a distance of fifty radii and the inward facing shock is at forty radii. The inward facing shock accelerates inward, gaining strength due primarily to cylindrical convergence.

7. The detonation products stop expanding and begin to contract when the shock reaches 100 charge radii. The inward moving shock reaches the axis of symmetry when the air shock reaches 130 charge radii (Figure 1). Upon reaching the center the shock reflects to a pressure greater than exists in the air shock (Figure 2). The reflected shock moves outward and rapidly decays (Figure 3). Other minor shocks continue to reverberate as the air shock advances and decays.

8. It is the formation of the ring of detonation products which causes the small impulse and short duration at small radii. The overpressure impulse and duration increase at larger radii because the detonation products reach their maximum radius and the inward moving shock spreads the energy inward from the high density ring of detonation products.

Problem – 5.0002
Time   – 4.500×10^{-3} sec
Cycle   – 11785.0
Maximum – 5.5488×10^{5} Pa
Minimum – -1.0106×10^{5} Pa

Radius of
Detonation Products

Air Shock Front

50 Charge Radii

100 Charge Radii
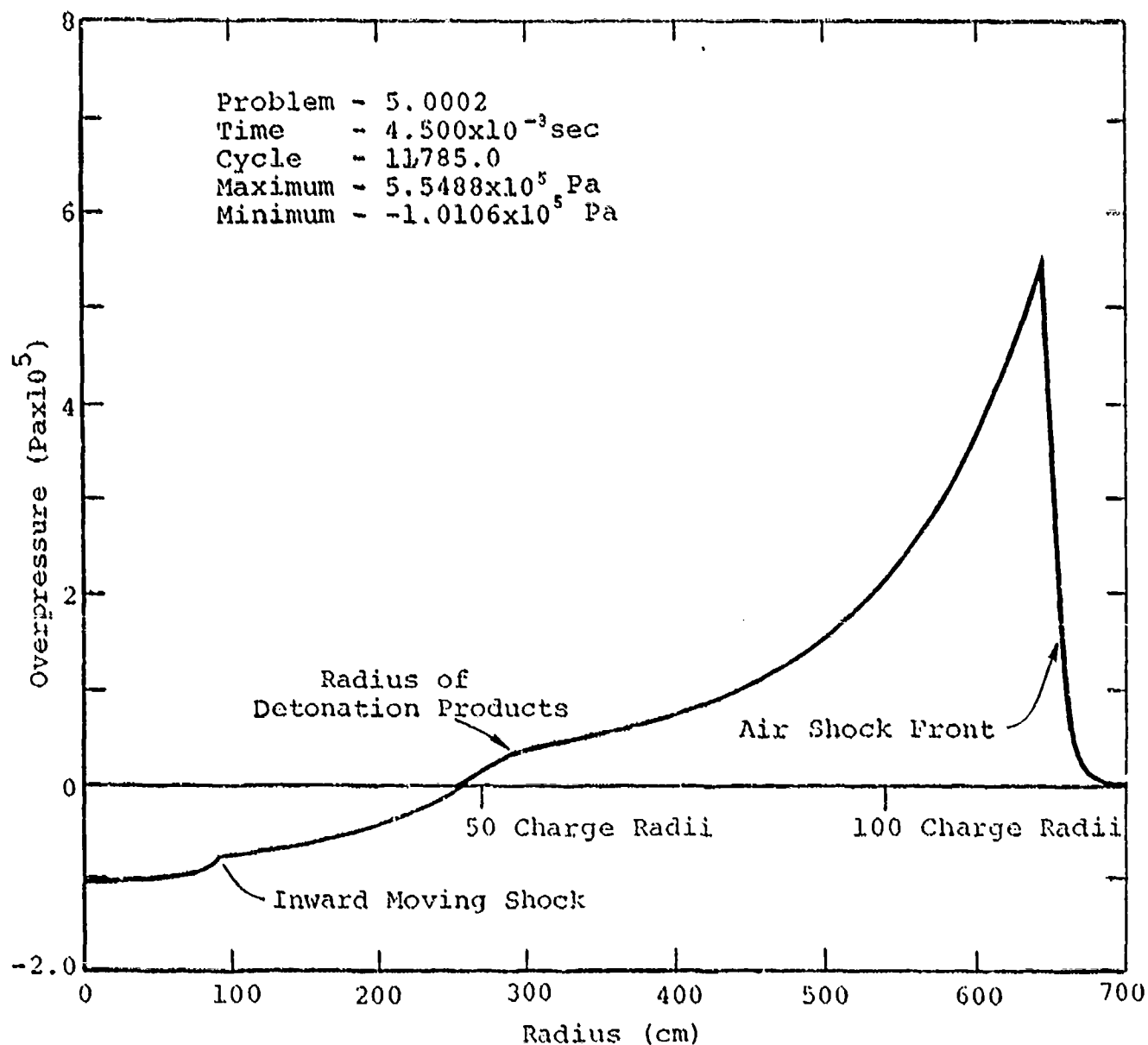
Inward Moving Shock

FIGURE 1.   Overpressure versus Ground Range
Line–Charge Calculation 15.12 kg/m

8
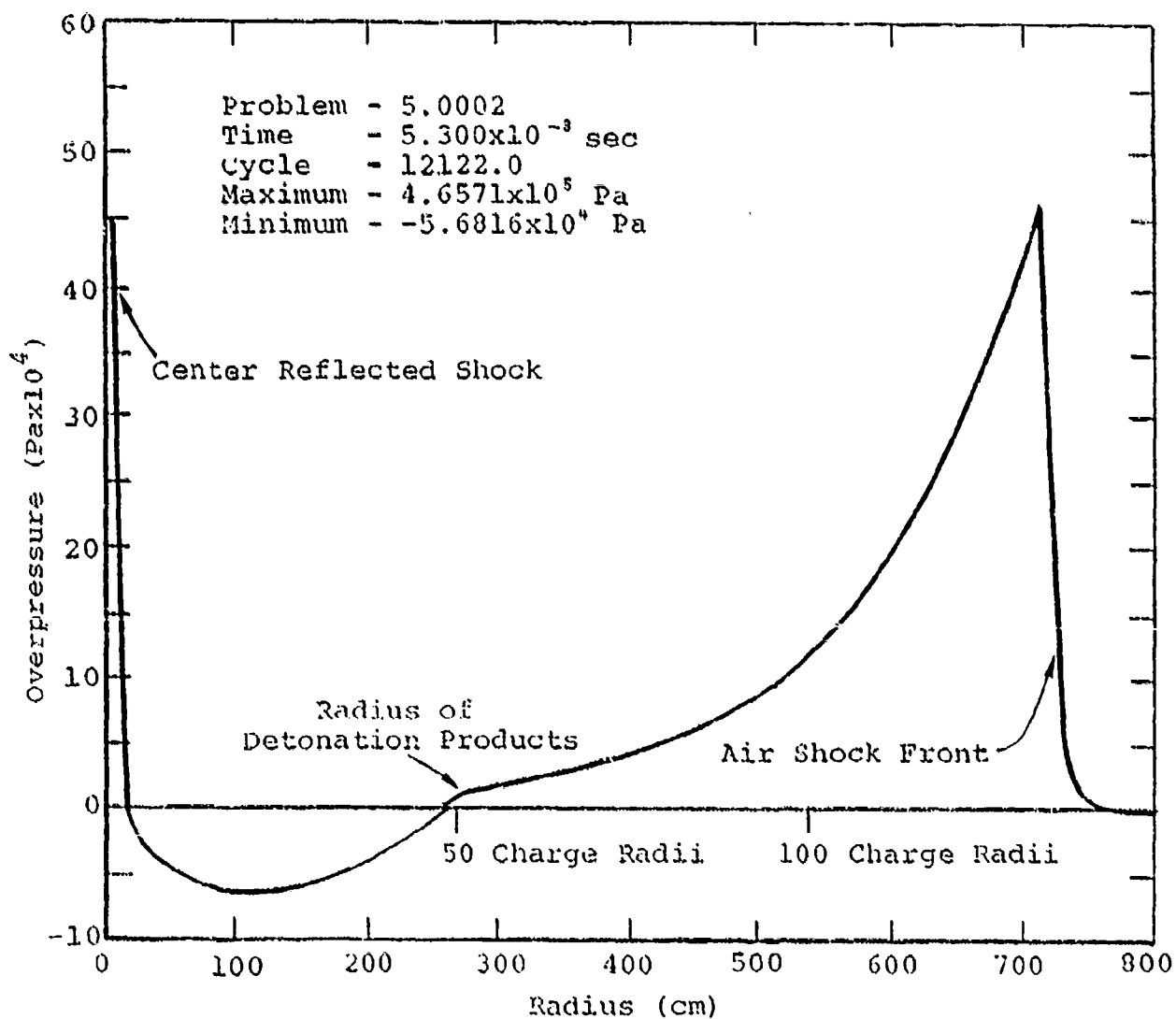
FIGURE 2. Overpressure versus Ground Range
Line-Charge Calculation 15.12 kg/m

Problem – 5.0002
Time – 6.500×10^{-3} sec
Cycle – 12536.0
Maximum – 3.7217×10^5 Pa
Minimum – -2.6277×10^4 Pa

Center Reflected Shock

Radius of Detonation Products

Air Shock Front

50 Charge Radii   100 Charge Radii

FIGURE 3.   Overpressure versus Ground Range
Line–Charge Calculation 15.12 kg/m

10

Airblast Characteristics

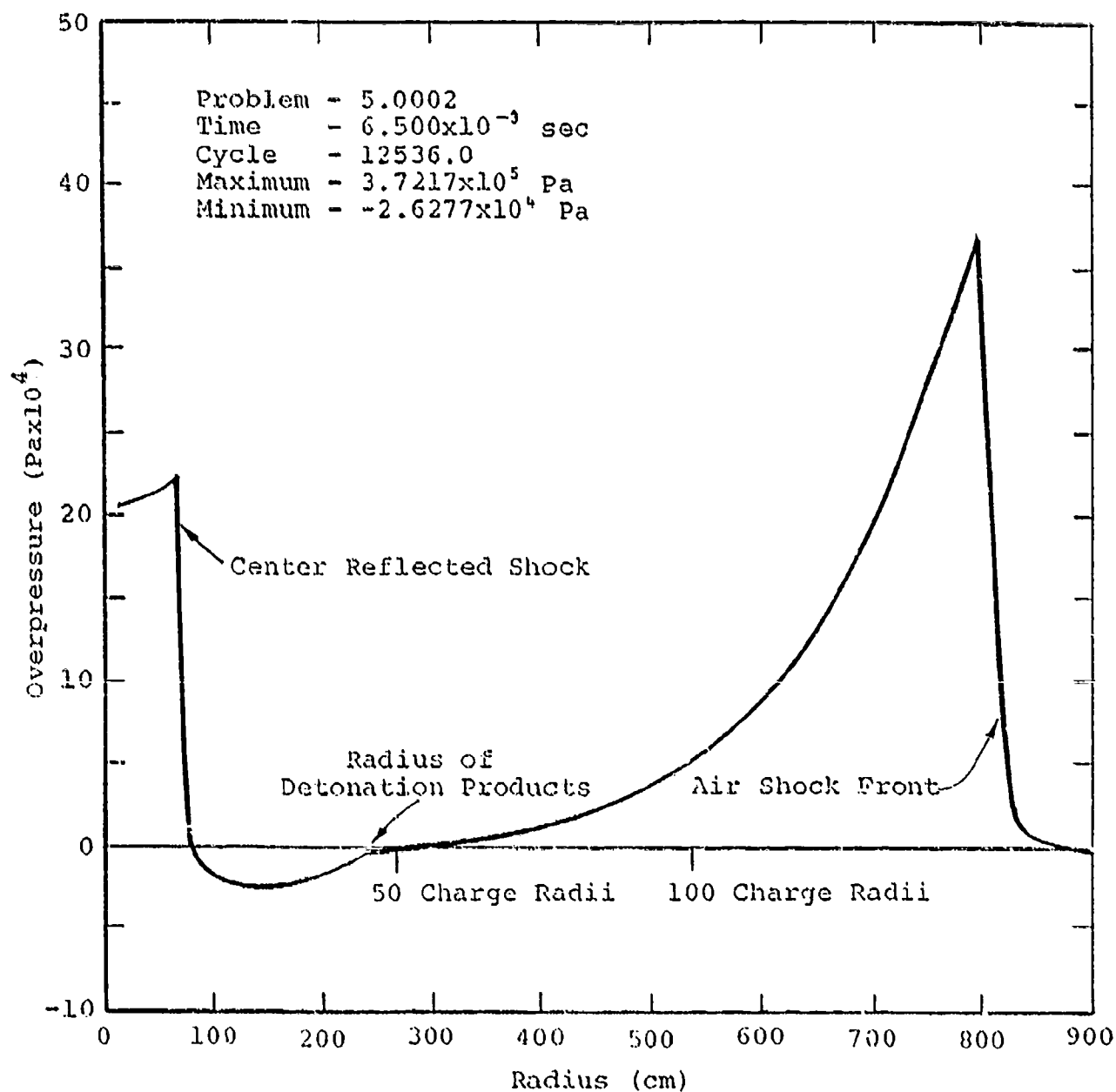9.   An important characteristic of the line charge is observed when plotting positive phase overpressure impulse as a function of radius (Figure 4). For a charge density of 7.56 kg/m, the experimental data reveals an impulse "well" centered at about 1 m (the extent of the skip zone). A peak occurs at 3 to 4 m before the impulse falls off again.

10.   SAP Problem 5.0002 is the first line-charge calculation that was made. It is compared to the data in Figures 4 and 5. The charge density was doubled in the calculation to simulate a detonation on a perfectly reflecting surface. Although the calculation falls below the data, the same characteristic decrease in impulse is seen, now centered at about 0.7 m. The corresponding peak occurs at just under 3 m.

11.   A study of the overpressure positive phase duration versus radius reveals an important line-charge characteristic (Figure 5). The prominent decrease in duration, starting at a radius of about 0.4 m and extending to about 1.8 m, with a minimum at 1.2 m, was not readily apparent in the experimental data. A noticeable phase difference is apparent between the impulse and duration minima. This is due to the overpressure waveform shape at the two points. Figure 6 is the overpressure time history from the calculation at 0.749 m from the charge center. Overpressure positive phase duration is defined as the difference in shock arrival time to the time at which the overpressure falls below zero. In this region, the waveform is characterized by a high-pressure spike followed by a long "tail" of low but positive overpressure. As the shock moves out radially, the ring of compressed air encircling the detonation products begins to stretch out and drop in pressure. The detonation products follow closely behind the shock and the drop off in pressure occurs abruptly at the inside edge. This behavior characterizes the overpressure waveform at 1.284 m in
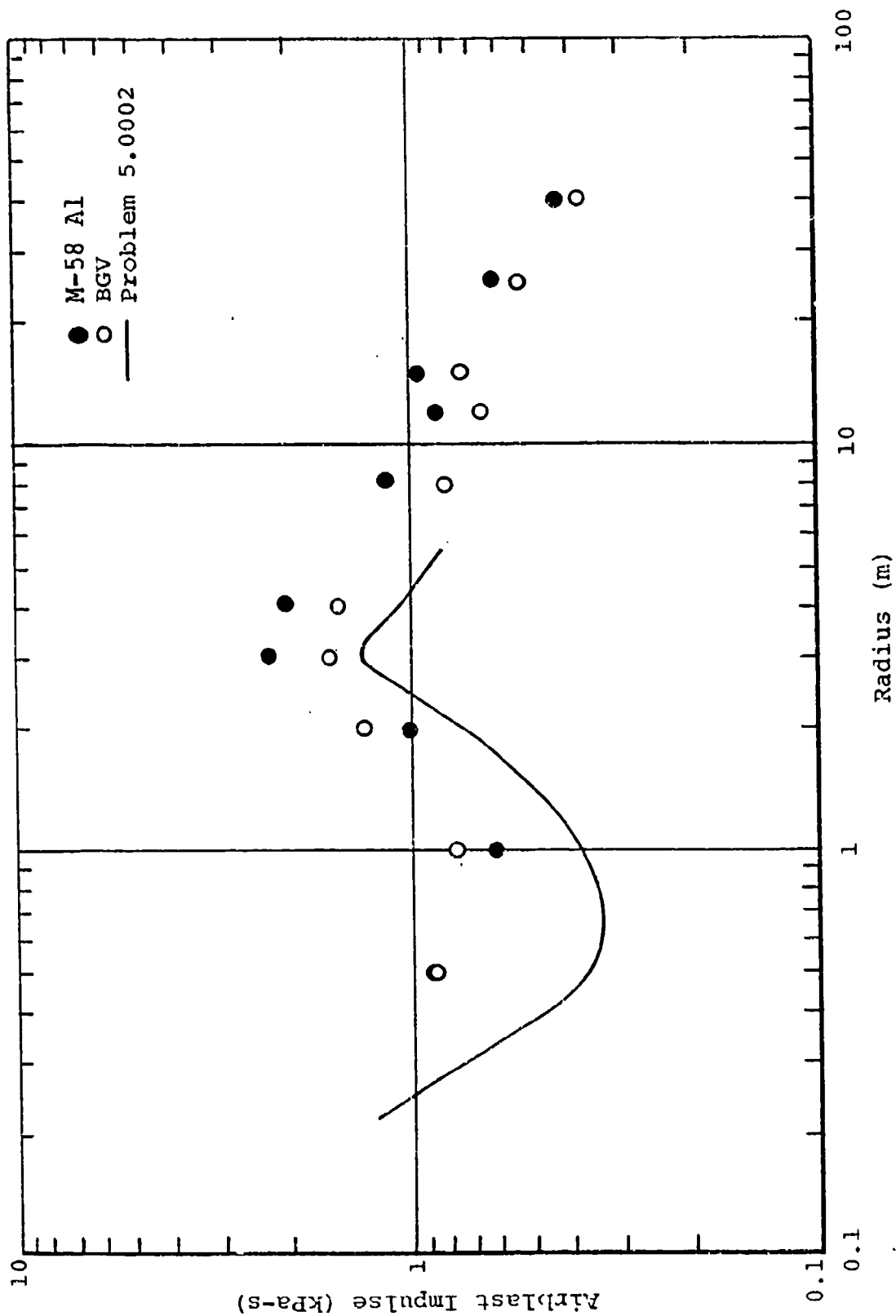
FIGURE 4. Averaged Airblast Impulse versus Transverse Distance from Line-Charge Center (M-58 Al and BGV, 30.48-m Charge Segments).
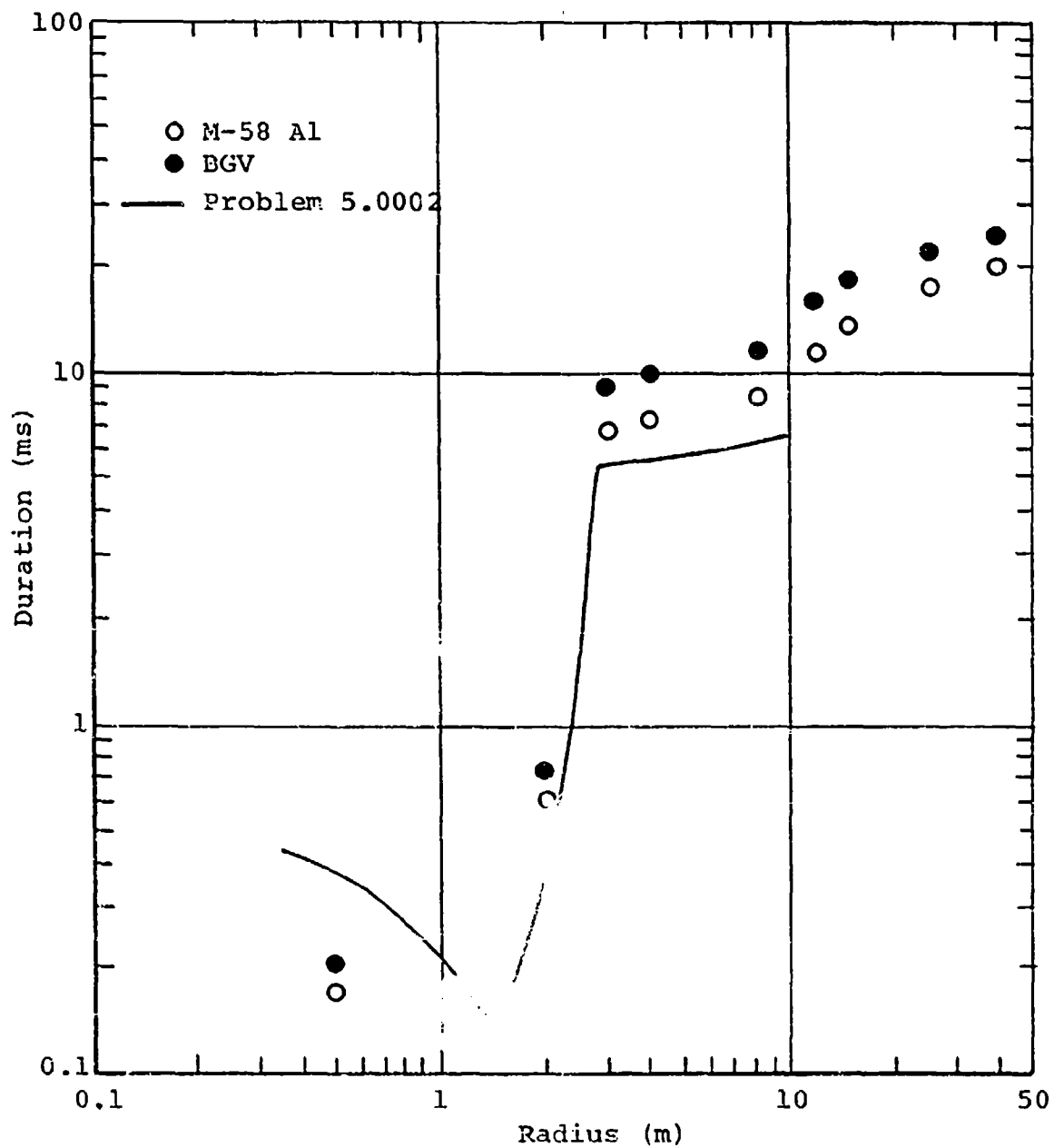
FIGURE   Surface Airblast Pressure Positive Phase
           Duration (Initial Pulse) versus Transver e
           Distance from Line-Charge Center (M-58 A_
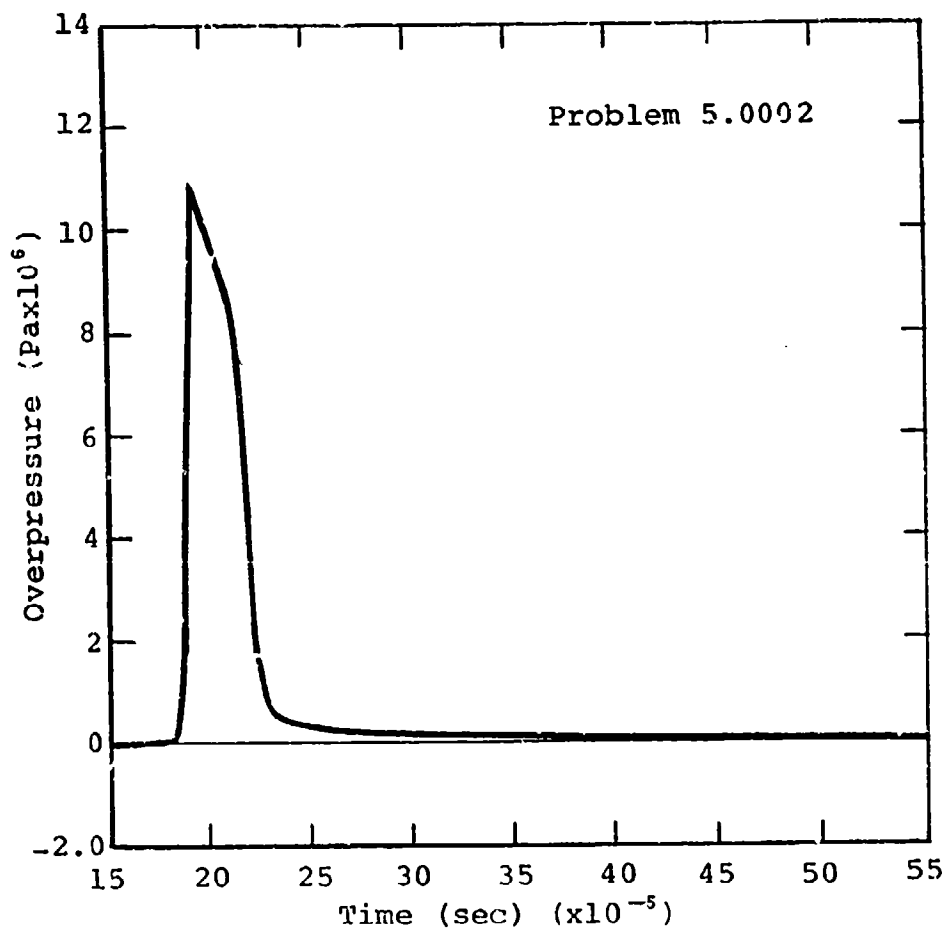   and BGV, 30.48-m Charge Segments)

13

FIGURE 6.   Overpressure versus Time
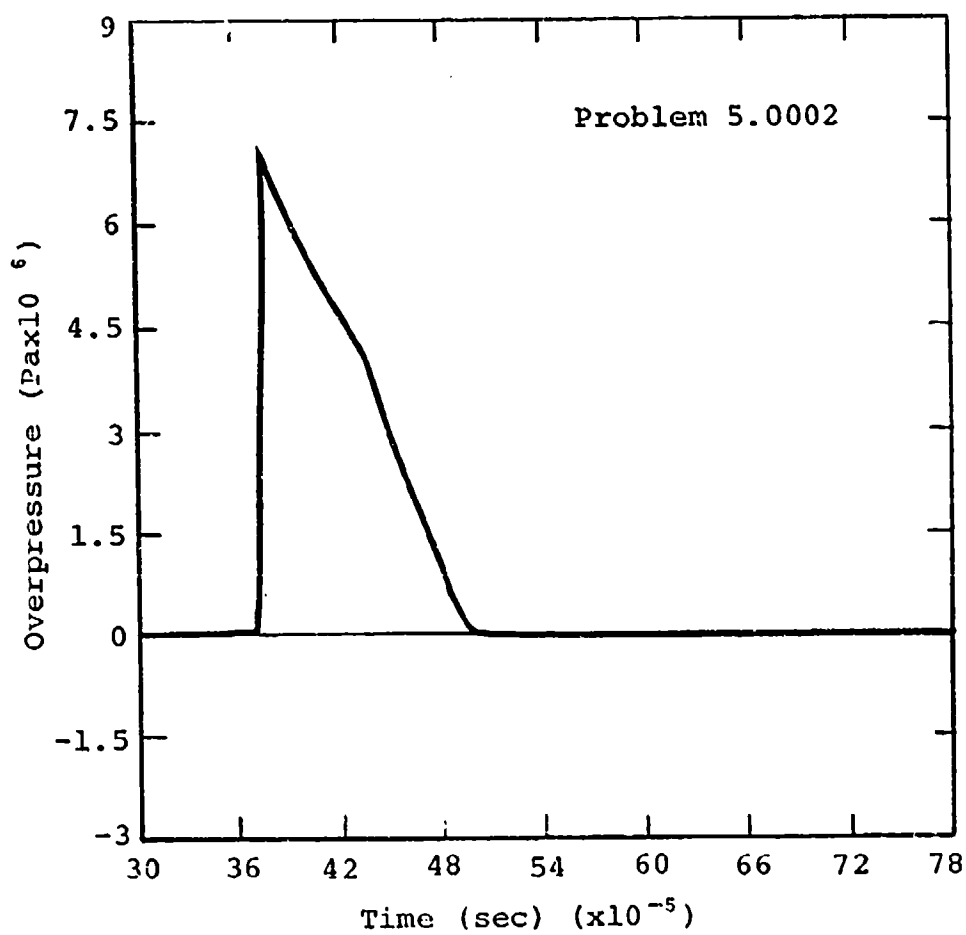   at 0.749-m Radius

14

FIGURE 7.   Overpressure versus Time
at 1.284-m Radius

15

Figure 7. In spite of the shorter duration, a larger impulse results because of the waveform shape.

12. The consistency between experiment and calculation is further demonstrated by the results in Figure 8. Here, the peak overpressure from the calculation falls along the BGV data to a radius of 6 m. No peculiarities in the overpressure profile are apparent in either experimental or calculational data.

13. Overpressure versus time comparisons of the calculation with experimental data are shown in Figures 9, 10, and 11. The experimental data show some gage noise, oscillation and overshoot. The calculation shows the arrival of the expanded detonation products as a sudden drop in overpressure at the 1- and 2-m stations. This is because the calculation models the interface as a boundary and does not allow mixing of the air with detonation products. The detonation products do not reach a distance of 3 m, therefore the comparison at that range shows a classical air shock decay in both experiment and calculation.

Calculation Variations

14. Three other calculations were run with variations in detonation treatment, density and initial detonation energy. Problem 5.0003 treated the detonation by allowing a cylindrical detonation wave to advance radially outward through the explosive. This procedure is further described in PART III. Problem 5.0004 was initiated with a uniform detonation energy of 5.86×10^{13} ergs/kg (as opposed to 5.155×10^{13} ergs/kgm in Problem 5.0002) to determine the effects of a higher-energy explosive. The third calculation, Problem 5.0001, used an increased charge density of 23.01 kg/m. The purpose of Problem 5.0001 was to approximate a high-energy explosive uniformly mixed with 34 percent inert materials.

15. Peak overpressures versus radius from all three calculations are compared with those of Problem 5.0002 in Figure 12.
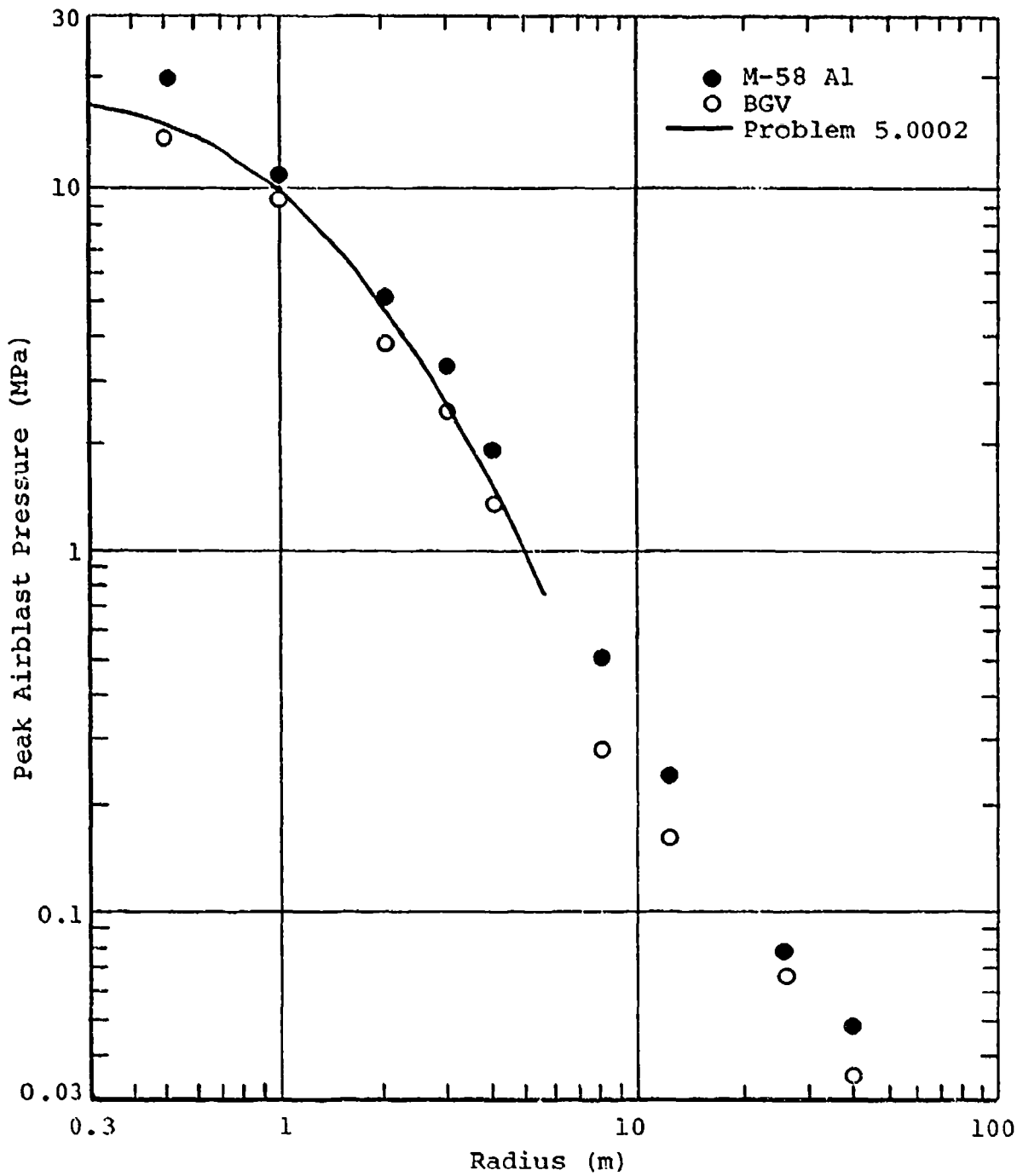
16

FIGURE 8. Averaged Surface Airblast Pressure versus Transverse Distance from Line-Charge Center (M-58 Al and BGV, 30.48-m Charge Segments)
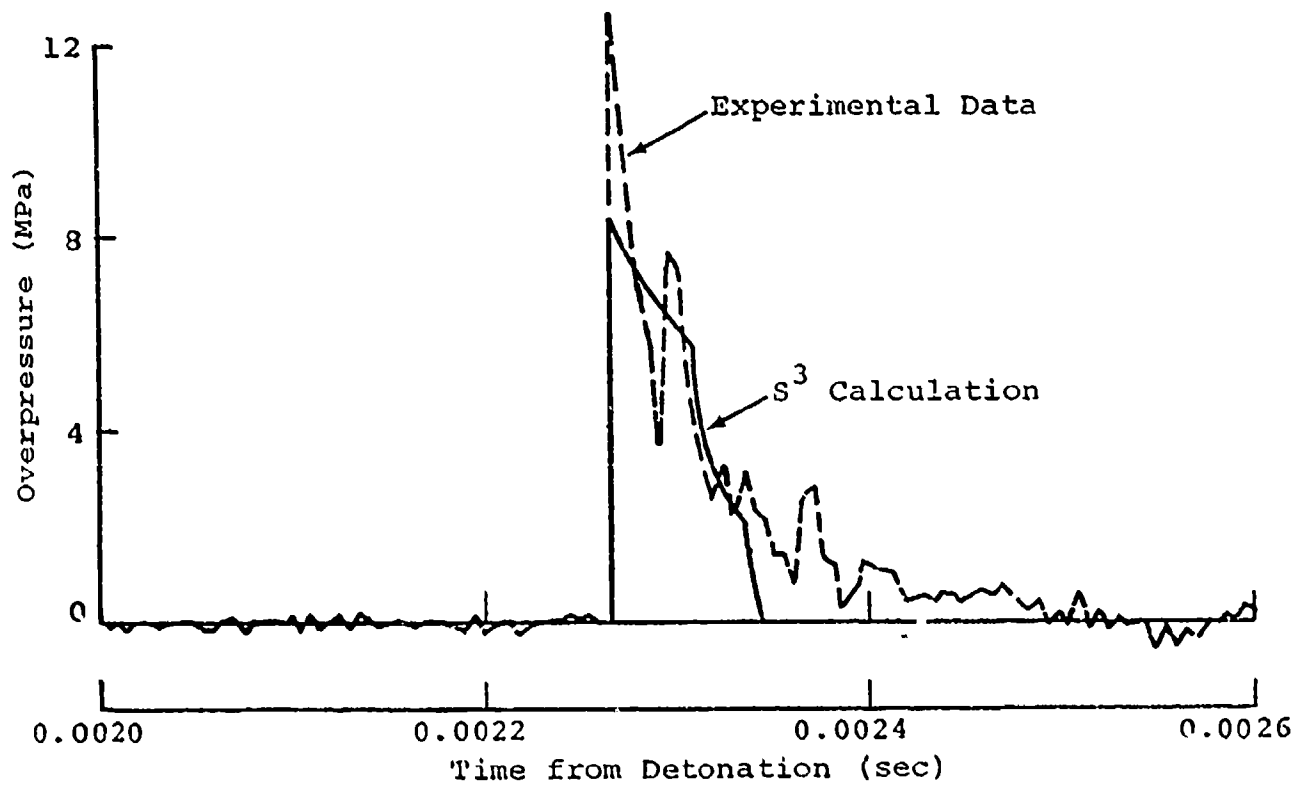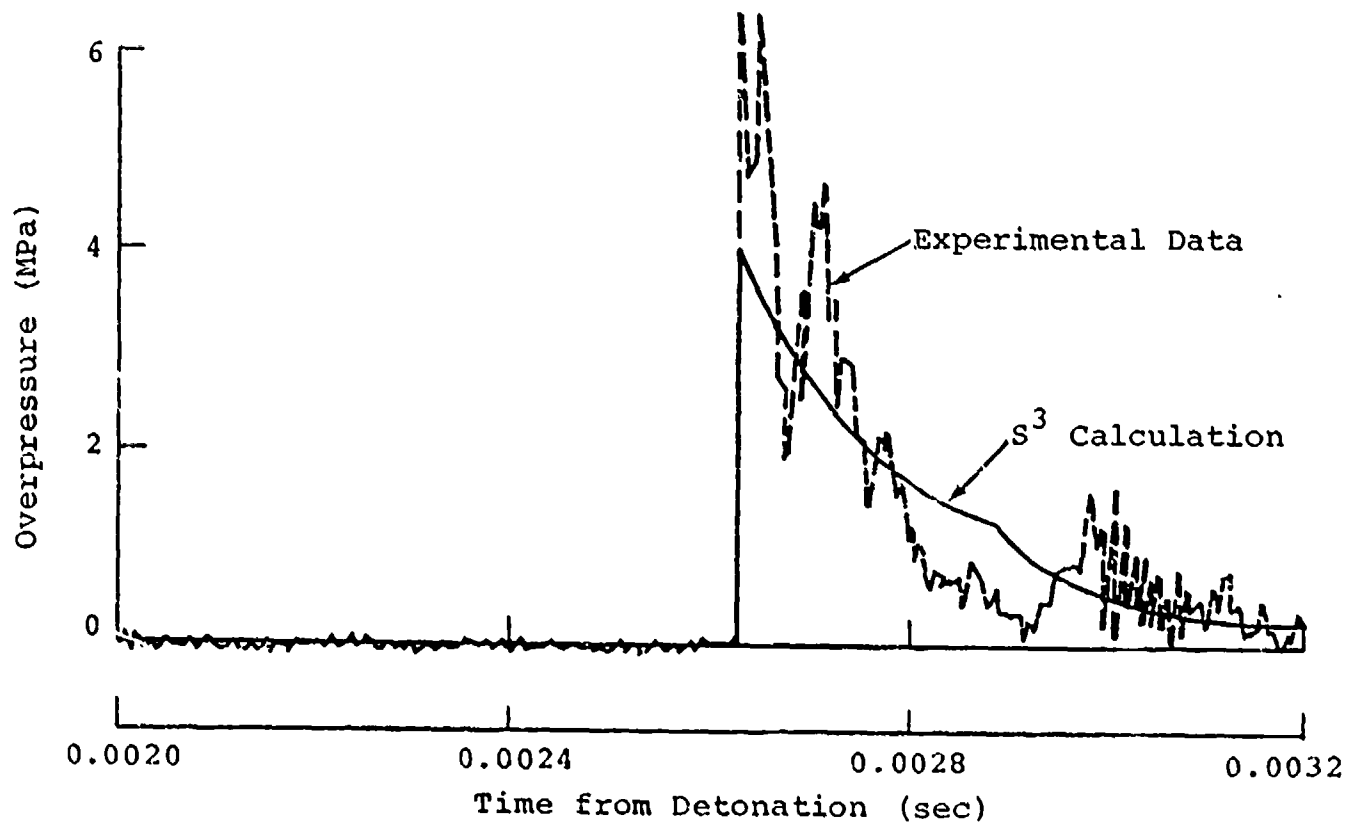
FIGURE 9. Overpressure versus Time - Event 2

R = 1 m

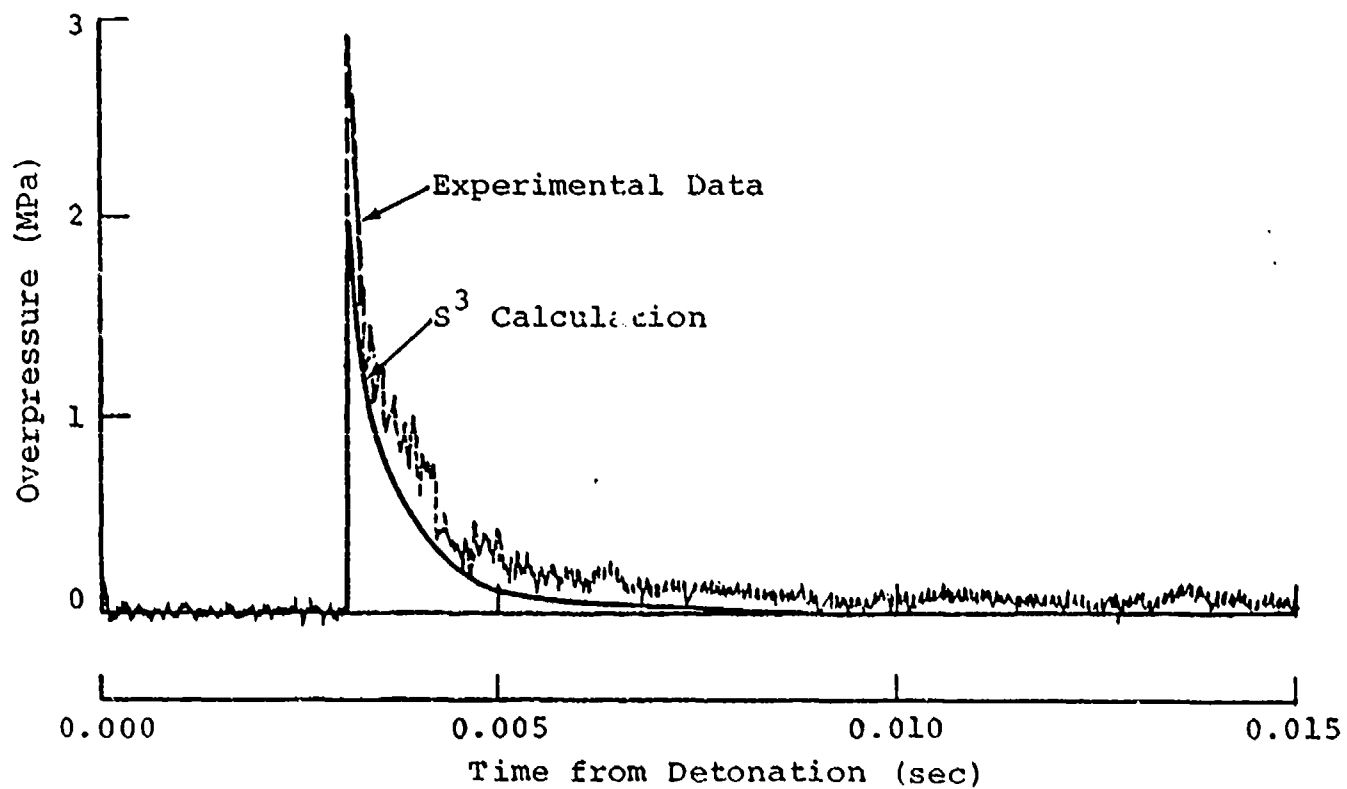18

FIGURE 10.   Overpressure versus Time – Event 2

R = 2 m

FIGURE 11.   Overpressure versus Time – Event 2
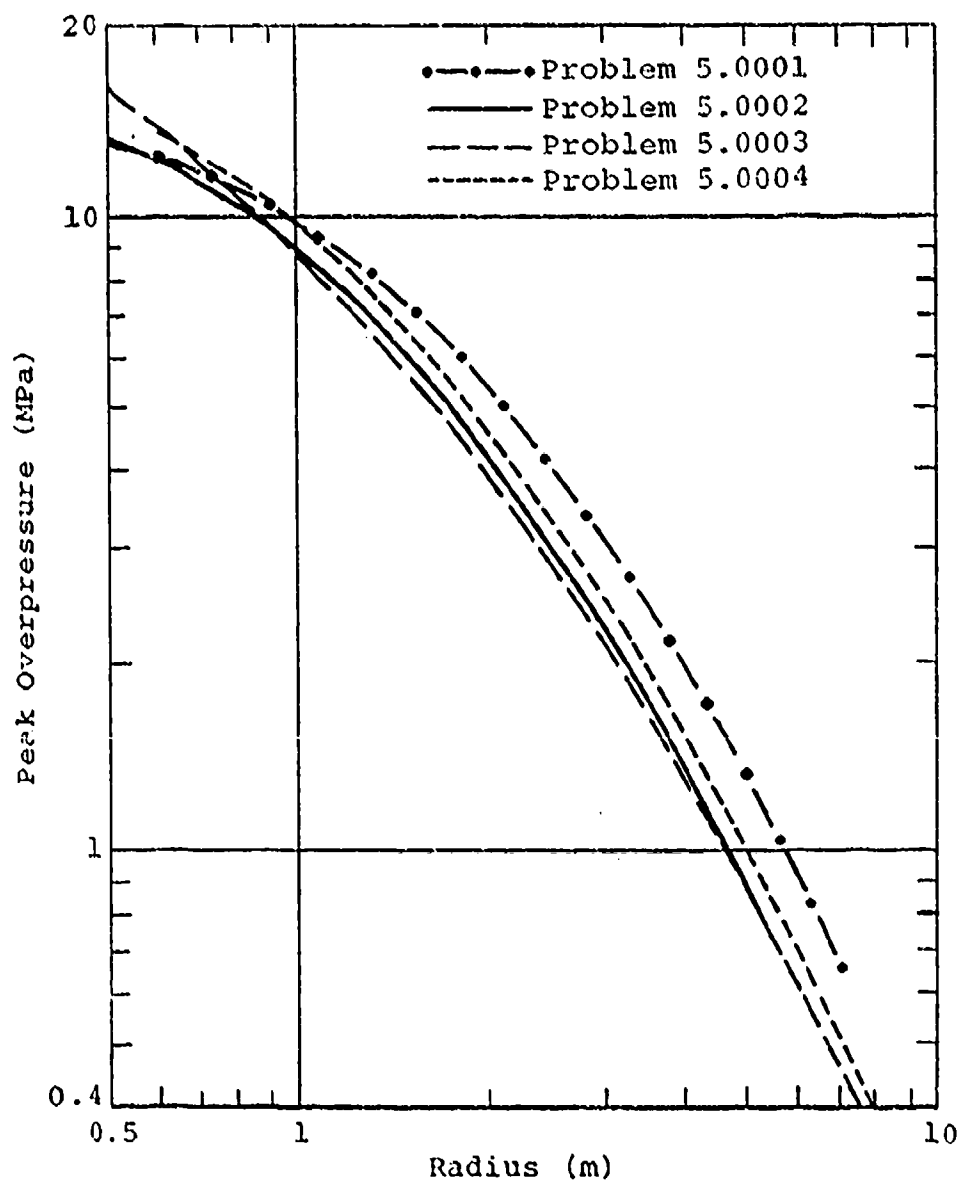R = 3 m

FIGURE 12. Comparison of Overpressure for
Various Initial Conditions

Minor differences due to detonation treatment (Problems 5.0002 and 5.0003) are seen in this comparison. Slightly higher pressures from the burn calculation inside of 0.5 m result from the larger amount of kinetic energy generated by burning the explosive. Very little difference can be seen outside the 0.5 m radius.

16. Some enhancement is obtained by using the same amount of a higher-energy explosive (Problem 5.0004). An increase which scales as the square root of the energy density ratios was obtained as expected.

17. The presence of large amounts of inert material combined with a higher-energy explosive, as in Problem 5.0001, resulted in a noticeable increase in overpressure at radii beyond 1 m.

18. The ability of the code to closely model line-charge phenomena gives credence to previously questioned experimental data and confidence in the continuation of line-charge calculations. An understanding of the line-charge airblast characteristics was obtained from the calculations as well as a basis for comparison with future calculations. As previously mentioned, the main effort was to enhance the overpressure impulse within the region of the skip zone with a minor effect on airblast parameters at the greater radii. The increase in impulse can be achieved by increasing the overpressure positive phase duration in this region. PART III describes S^3's approach to the solution and includes a "directory" of calculations and their descriptions.

PART III.   CALCULATION DESCRIPTIONS

19.   A total of 12 line-charge calculations were made. The purpose of the first four calculations was to determine the ability of the code to simulate a line-charge. The final eight are considered to be line-charge-improvement calculations. A breakdown and brief summary of each calculation follows.

20.   In order to simulate charge characteristics in the code, several simplifying assumptions had to be made. The charge was assumed to be an infinitely long, solid cylinder of 100 percent HE mass. This assumption ignores end effects of the charge and any inert mass surrounding or inside the charge. The input charge mass was twice that of the experimental mass in order to simulate a surface detonation on a perfectly reflecting surface. The detonation of the charge was treated in two ways. The first method simulates the situation if a planar detonation wave travels axially down the charge. For calculations using this method, the initial HE region is a high-energy density isothermal region of burned HE material. The second treatment simulates a cylindrical detonation wave starting at the inner HE radius and burning outward in the radial direction. The initial conditions in the HE region include an inner zone of burned pentolite (properties identical to those in the axial detonation calculations) and surrounding zones of low energy, unburned HE material at ambient air pressure. A calculation using this treatment will be referred to as a "burn" calculation, whereas the convention for the axial detonation will be "isothermal".

21.   Both detonation treatments are correct. It is not clear, however, which treatment models the experimental situation more closely. The most appropriate treatment is dependent on where and how the charge is detonated. A representation of the two treatments is shown in Figures 13 and 14.

22.   All calculations can further be divided into two groups based upon the charge configuration:

High-Energy Isothermal
Explosive Material

$\rho = 1.66 \times 10^3$ kg/m^3
$E = 5.15 \times 10^{13}$ ergs/kg

Unburned HE Material
$E = 1.0 \times 10^{11}$ ergs/kg
$\rho = 1.66 \times 10^3$ kg/m^3

5.35 cm
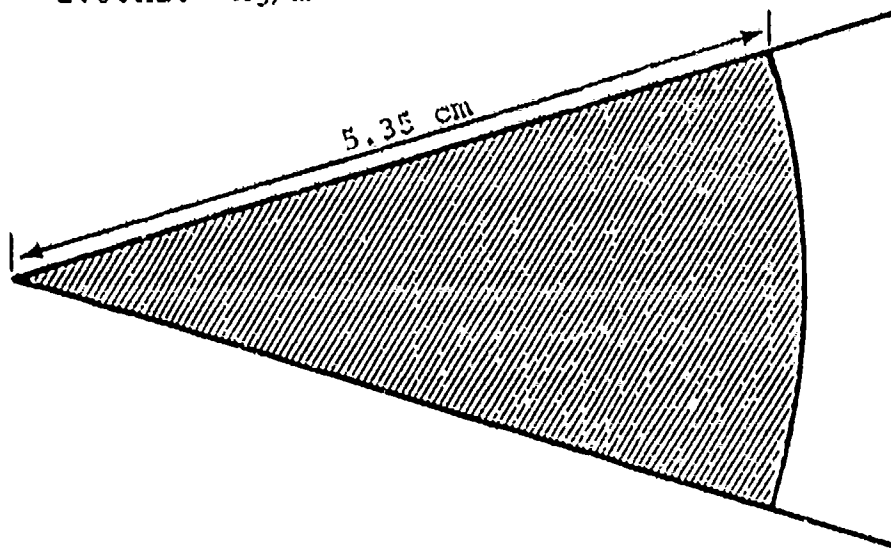
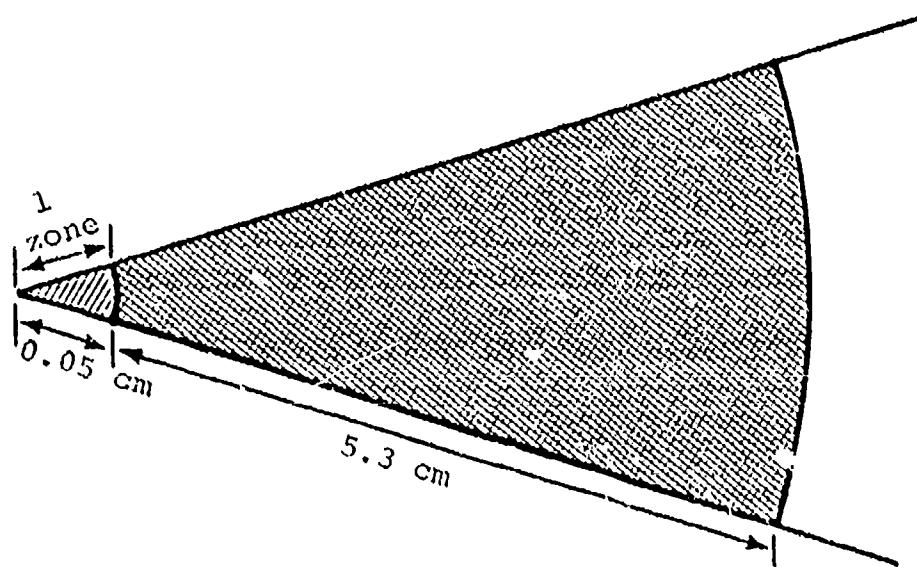FIGURE 13.   Axial Detonation (Isothermal)

1
zone

0.05 cm

5.3 cm

FIGURE 14.   Radial Detonation (Burn) Charge Configuration

24

a. The "solid" charge.

b. The "hollow-center" charge.

Table 1 lists the solid-charge calculations and pertinent information regarding initial conditions for each. Table 2 describes the hollow-center-charge calculations.

Calculation Zoning

23. The solid-charge calculations used a solid cylinder of HE surrounded by ambient air (Figure 15). The HE region is made up of approximately 100 zones of 0.5 mm size. The charge is surrounded by ambient sea-level air. The first few zones at the HE air interface are large and decreasing in size. This is necessary due to the compression of the zones as the shock passes through. These decreasing zones are followed by about 100 to 150 zones of constant size and then increasing size zones at a constant expansion ratio out to a radius of about 14 m. Problem 5.0012 is the only deviation from the above configuration among the solid charge calculations. A 2-cm layer of low energy, dense air surrounds the charge in Problem 5.0012, with ambient air in the rest of the grid. This modification was made to determine the effect of surrounding the charge with a layer of dense, inert material.

24. The basic configuration for the hollow-center charges is shown in Figure 16. The center four to five zones contain air at ambient pressure, with the volume of this center region varied in three different calculations (Problems 5.0006, 5.0007, and 5.0008). From thirty to sixty zones of HE, depending on the calculation, surround the air zones. The HE region is again surrounded by the decreasing, constant, and then increasing ambient air zones. Problem 5.0013 is classified as a hollow-center calculation, yet has a slightly varied charge configuration (Figure 17). This configuration is referred to as a "double charge". The center zones are of HE surrounded by two

25

TABLE 1

Solid-Charge Calculations

Problem Number	Charge Density (kg/m)	Charge Radius (m)	Detonation Treatment	Variations
5.0001	23.01	0.066	Isothermal	None
5.0002	15.12	0.0535	Isothermal	None
5.0003	15.12	0.0535	Burn	None
5.0004	15.12	0.0535	Isothermal	Initial charge energy density of 5.86×10^{13} ergs/kg
5.0012	15.12	0.0535	Isothermal	0.02-m layer of air surrounding the charge surface air layer properties: $\rho = 100$ kg/m^3 $E = 2.43 \times 10^{10}$ ergs/kg

TABLE 2

Hollow-Charge Calculations

PART A

Problem Number	Charge Density (kg/m)	Inner Charge Radius (m)	Outer Charge Radius (m)	Center Vol.to Charge Vol.Ratio	Detonation Treatment	Variations
5.0006	15.12	0.0535	0.07558	1:1	Burn	None
5.0007	15.12	0.03779	0.06545	0.5:1	Burn	None
5.0008	15.12	0.07558	0.09257	2:1	Burn	None
5.0009	15.12	0.0535	0.07558	1:1	Isothermal	None
5.0010	15.12	0.0535	0.07558	1:1	Isothermal	Water cent calculations. Conditions of water in charge center are as follows: $P = 1.0127 \times 10^5$ Pa $\rho = 991.$ kg/m^3 $E = 6.4 \times 10^{11}$ ergs/kg
5.0011	15.12	0.0535	0.07558	1:1	Isothermal	High density, low-energy air in charge center at following conditions: $\rho = 100$ kg/m^3 $E = 2.43 \times 10^{10}$ ergs/kg

27

TABLE 2
(Continued)

Hollow-Charge Calculations

PART B

Problem Number	Charge Density (kg/m)	Radius of Inner HE Region (m)	Inner Radius of Outer HE Region (m)	Outer Radius of Outer HE Region (m)	Center Vol. to Charge Vol. Ratio	Detonation Treatment	Variations
5.0013	15.12	0.03779	0.05779	0.06905	1:1	Isothermal	Double charge calculation. Region between the two HE regions is air at the following conditions: $\rho = 100$ kg/m^3 $E = 2.43 \times 10^{10}$ ergs/kg
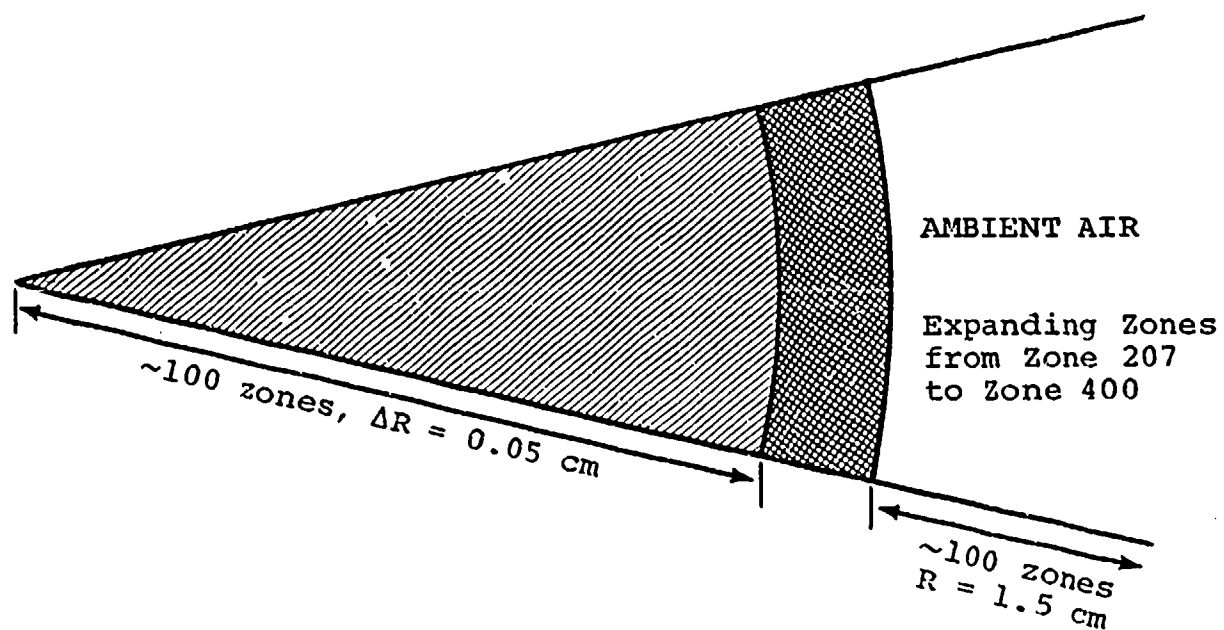
FIGURE 15.   SAP Solid Charge Initial Mesh Configuration

Explosive Material   15.12 kg/m

AMBIENT AIR   AMBIENT AIR

~5 zones

~30 zones
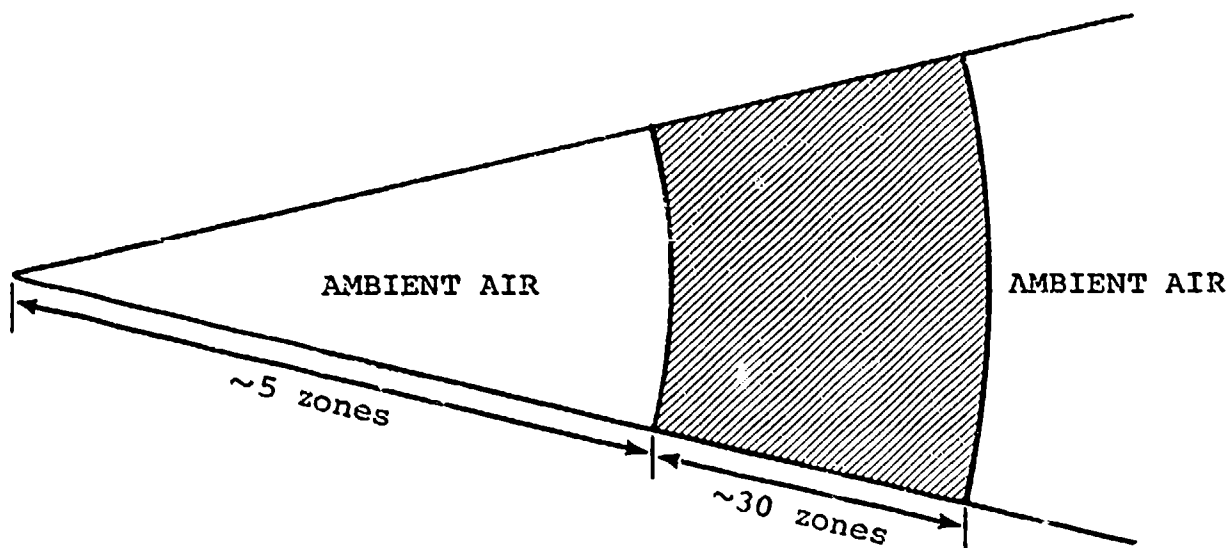
FIGURE 16.   SAP Hollow Charge Initial Mesh Configuration

30

Explosive Material   Double Charge Calculation
                            10 lb/ft Charge

Dense Air $\rho = 100$ kg/m^3
Energy $= 2.43 \times 10^{10}$ ergs/kg

7.56 kg/m

7.56 kg/m

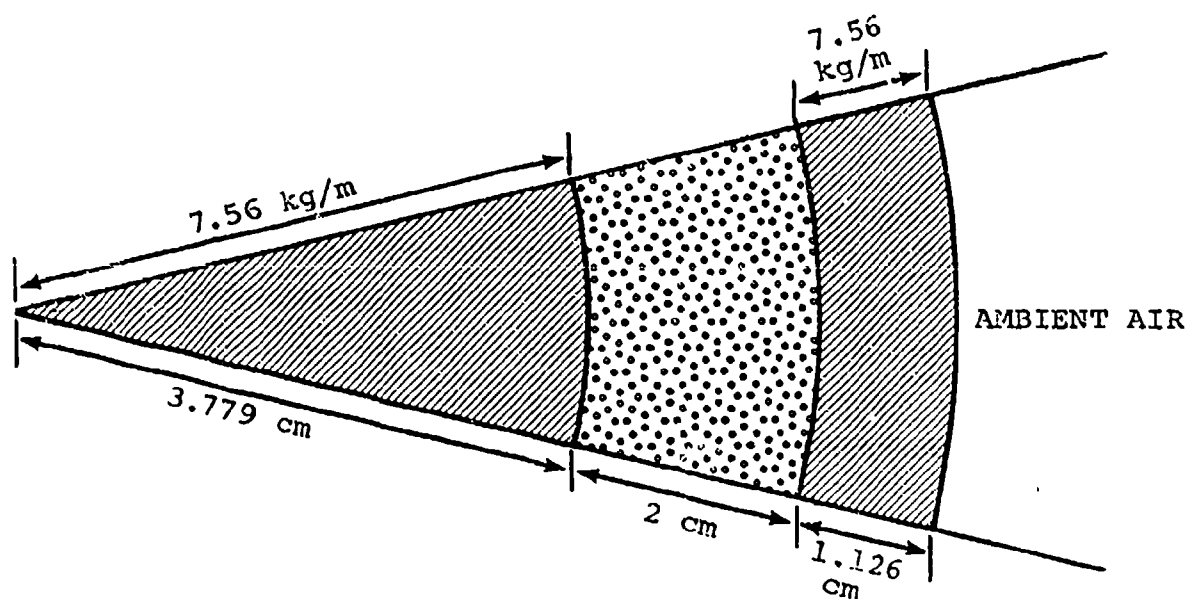AMBIENT AIR

3.779 cm

2 cm

1.126 cm

FIGURE 17.   SAP Problem 5.0013 Initial Mesh Configuration

zones of air and, in turn, surrounded by several more zones of HE. A low energy, dense air is used between the two HE regions to simulate the presence of a low density foam in this region. The final HE region is surrounded by ambient air out to a radius of just over 13 m.

25. Each of the calculations was run to a time when the overpressure positive phase was complete inside a minimum distance of 1.75 m. A complete set of station plots was made for each of the calculations. Tables and plots of peak parameters from each station were made for direct comparison. These are discussed in PART IV.

PART IV. CALCULATIONAL RESULTS

26. The hollow-center charge calculations were the first attempts at increasing the overpressure impulse. Stretching the ring of detonation products is the means by which the impulse should be increased. During the hollow-charge detonation, an inward moving shock is created by the detonation products as they move into the less dense air zones in the center of the charge. This shock will reflect from the center, pass through the ring of detonation products, now much wider than in the case of the solid charge, and catch up to the main shock, hopefully outside the skip zone. The stretched detonation product ring plus the additional reflected shock should yield a higher impulse in this region.

Hollow-Charge Calculations

27. Three separate calculations of this type were made, varying only the volume of air in the charge center. Problems 5.0006, 5.0007, and 5.0008 contained center volumes equal to one, one half, and two times the charge volume, respectively. Each calculation was carried out to a time at which the positive phase duration was complete inside 3 m.

28. The actual shock interactions can be seen by following the results of Problem 5.0006 in time.

29. Because Problem 5.0006 is a burn calculation, the initial overpressure versus radius profile shows a single zone of high-energy detonation products (Figure 18). As the HE burns to the outer surface, detonation products on the inner surface move inward, compressing the air in the center of the charge. A high-pressure shock is generated in the air which reflects off the center when the main air shock has reached a radius of 0.143 m (Figure 19). The reflected shock drops in pressure as it advances radially through the detonation products. The reflected shock reaches the outer HE-air interface when the
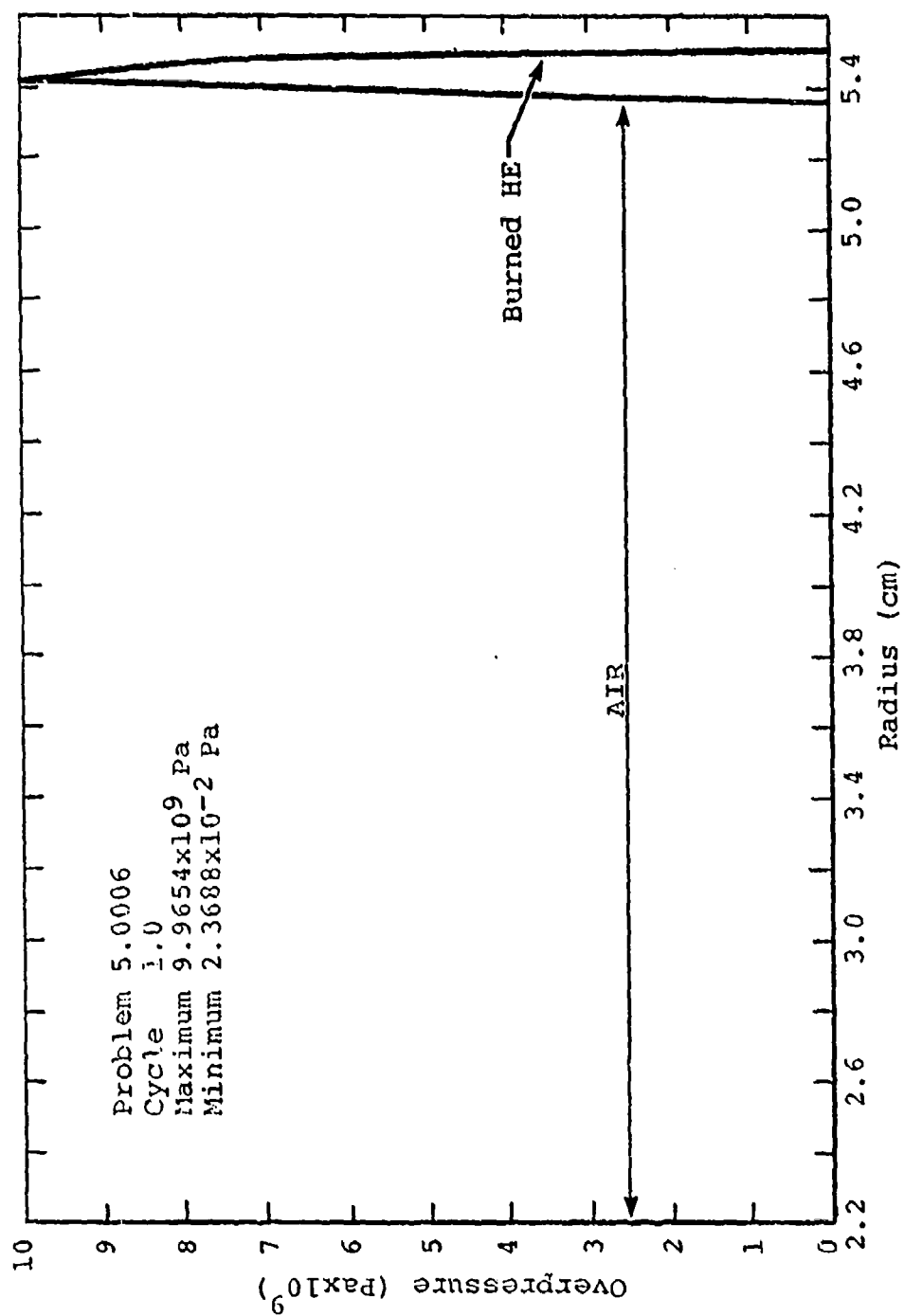
33

FIGURE 18. Initial Overpressure versus Radius at 0.0 sec

The figure shows a plot of Overpressure (Pa×10⁹) versus Radius (cm).

Plot annotations:
Problem 5.0006
Cycle 1.0
Maximum 9.9654x10⁹ Pa
Minimum 2.3688x10⁻² Pa

Labels: Burned HE, AIR

Problem 5.0306
Cycle   508.0
Maximum 1.9868x10^9 Pa
Minimum 2.4027x10^{-2} Pa
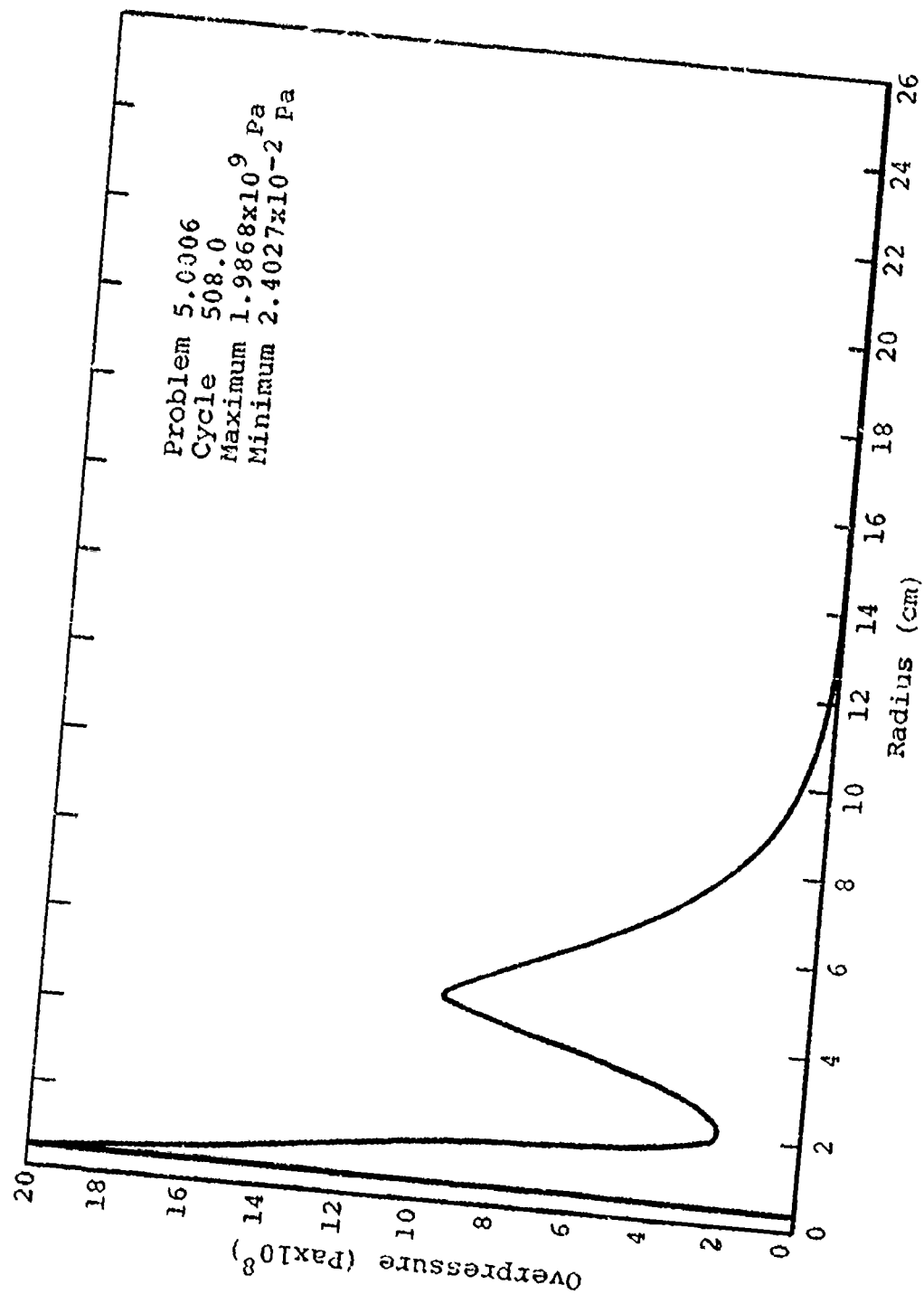
Overpressure (Pax10^8)

Radius (cm)

FIGURE 19. Overpressure versus Radius at 0.011 msec

main shock front is at a radius of 1.3 m (Figure 20). As the reflected shock moves into the air, it generates the large secondary pressure spike shown in Figure 21.

30. The time history results generated by this reflected shock are represented in Figures 22 and 23. The overpressure time history at 0.6 m in Figure 22 shows the reflected shock as a low amplitude secondary shock as it passes through the detonation products. It is the presence of this secondary shock which causes the increase in impulse at small distances. At a radius of 1.2 m (Figure 23), the reflected shock is outside the detonation products and produces a high amplitude, double peaked waveform.

31. At later times, a second reflected shock similar to that produced by the solid charge (as mentioned in PART II) can be seen reflecting from the charge center. This occurs at extremely late times and is not seen in the time frame of the experimental pressure time recordings.

32. A plot of peak overpressure versus radius for the three hollow-charge calculations (Problems 5.0006, 5.0007, and 5.0008) as compared to the solid-charge calculation (Problem 5.0003) is given in Figure 24. Overpressures are slightly higher inside 0.8 m for the hollow charges because the charge surface is closer to each station. As the main and inward moving shocks separate, a slight decrease in pressure below the solid charge data is seen. At a radius of 1.8 to 2 m, the pressure suddenly rises to the solid charge data marking the point where the reflected inward moving shock has caught up with the main shock. The distance at which the reflected shock catches up is dependent on the center charge volume: the smaller the volume, the earlier the shock catches up. Beyond the joining of the two shocks, peak pressures are in close agreement with the solid charge data.

33. The most encouraging results of these calculations are shown in Figure 25. Here, a definite enhancement is seen
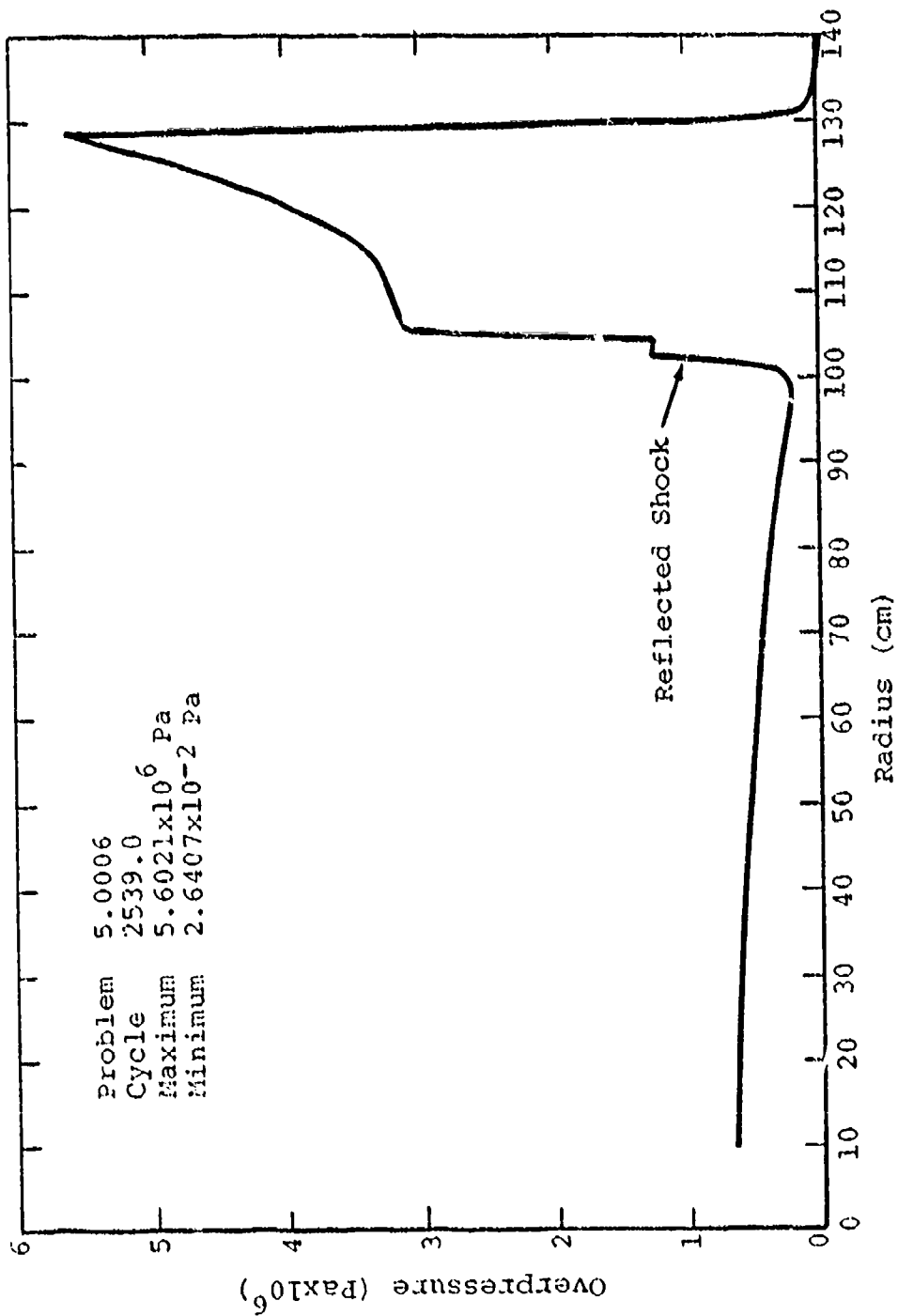
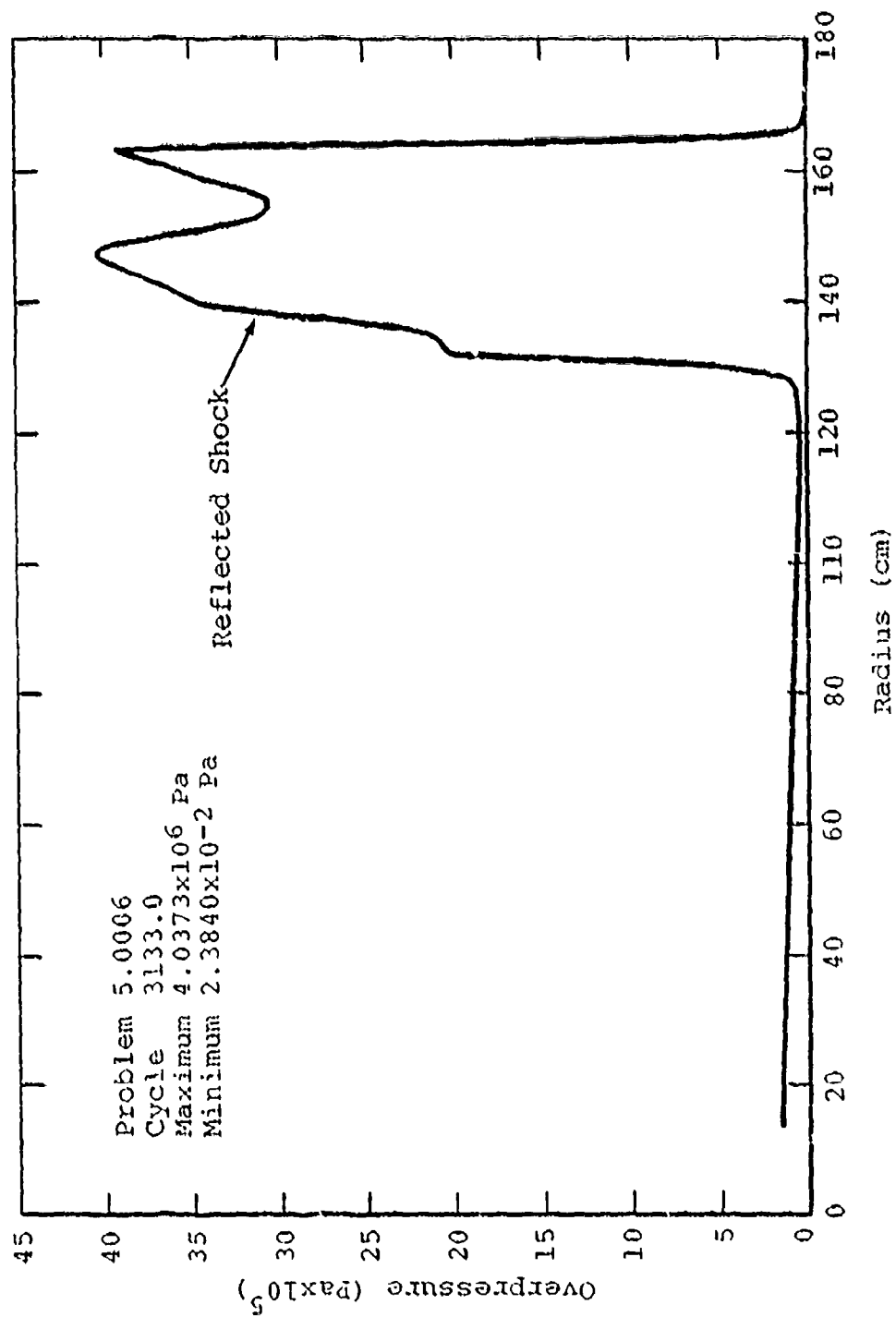FIGURE 20. Overpressure versus Radius at 0.34 msec

FIGURE 21. Overpressure versus Radius at 0.5 msec

Problem 5.0006
Cycle 3133.0
Maximum 4.0373x10⁶ Pa
Minimum 2.3840x10⁻² Pa

Reflected Shock
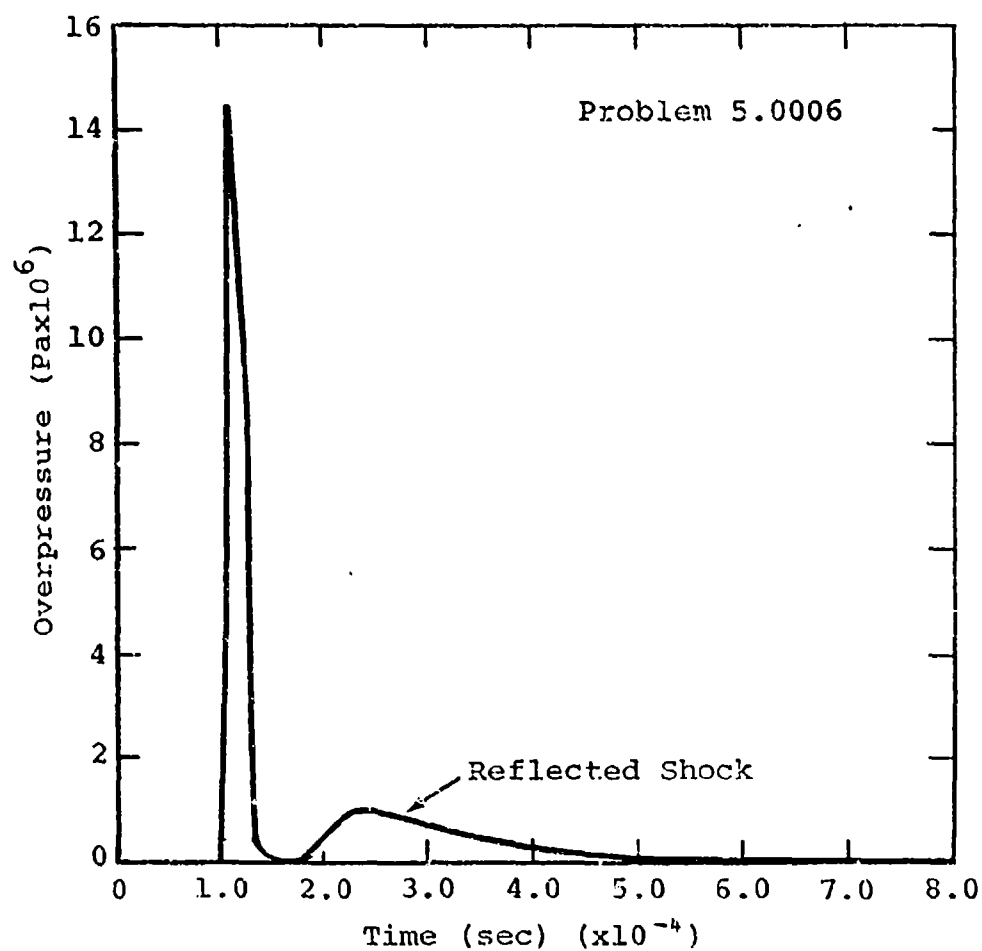
Overpressure (Pax10⁵)

Radius (cm)

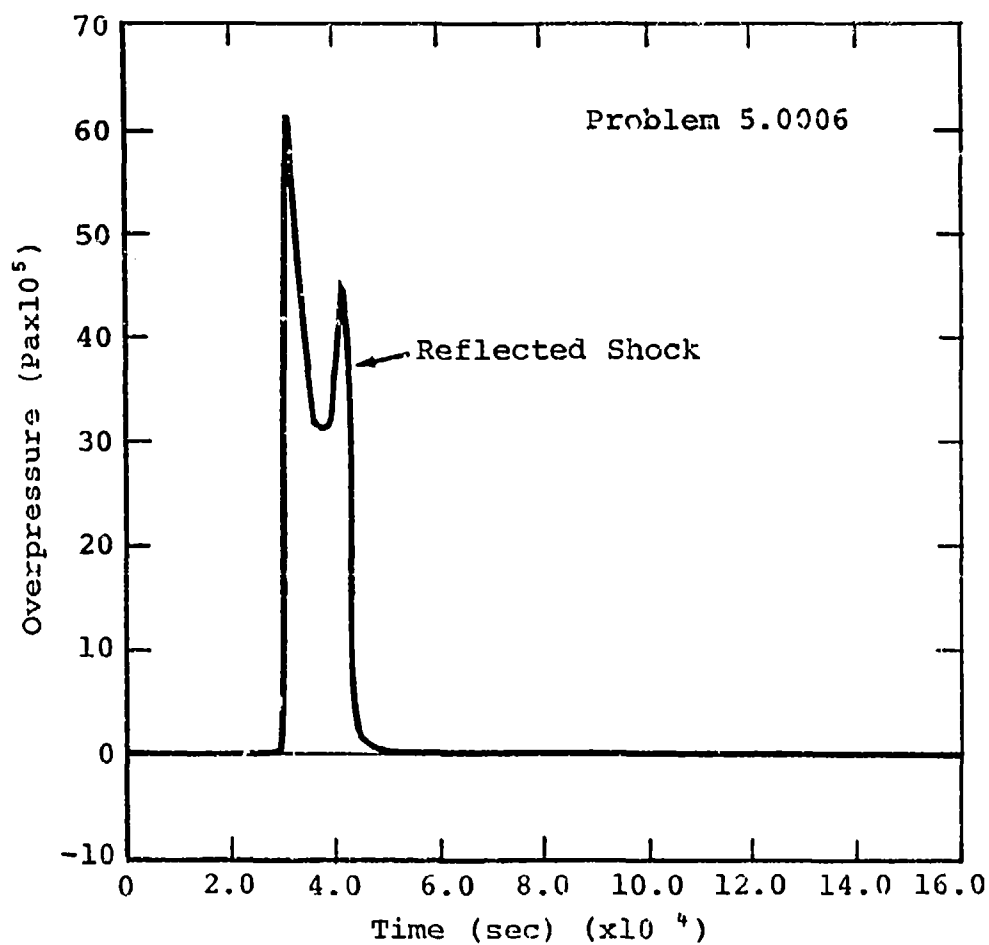FIGURE 22. Overpressure versus Time at 0.6-m Radius

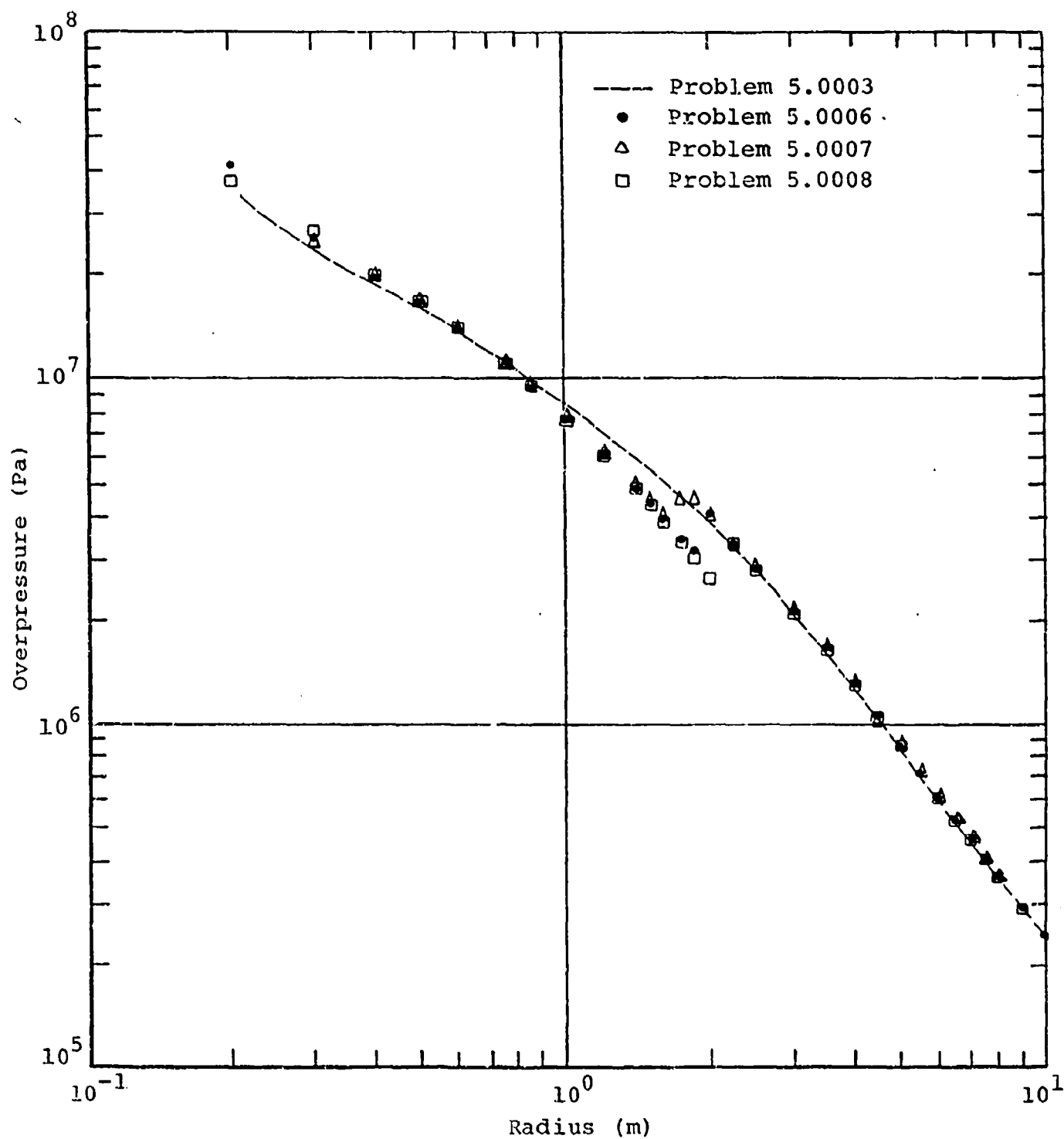FIGURE 23. Overpressure versus Time at 1.2-m Radius
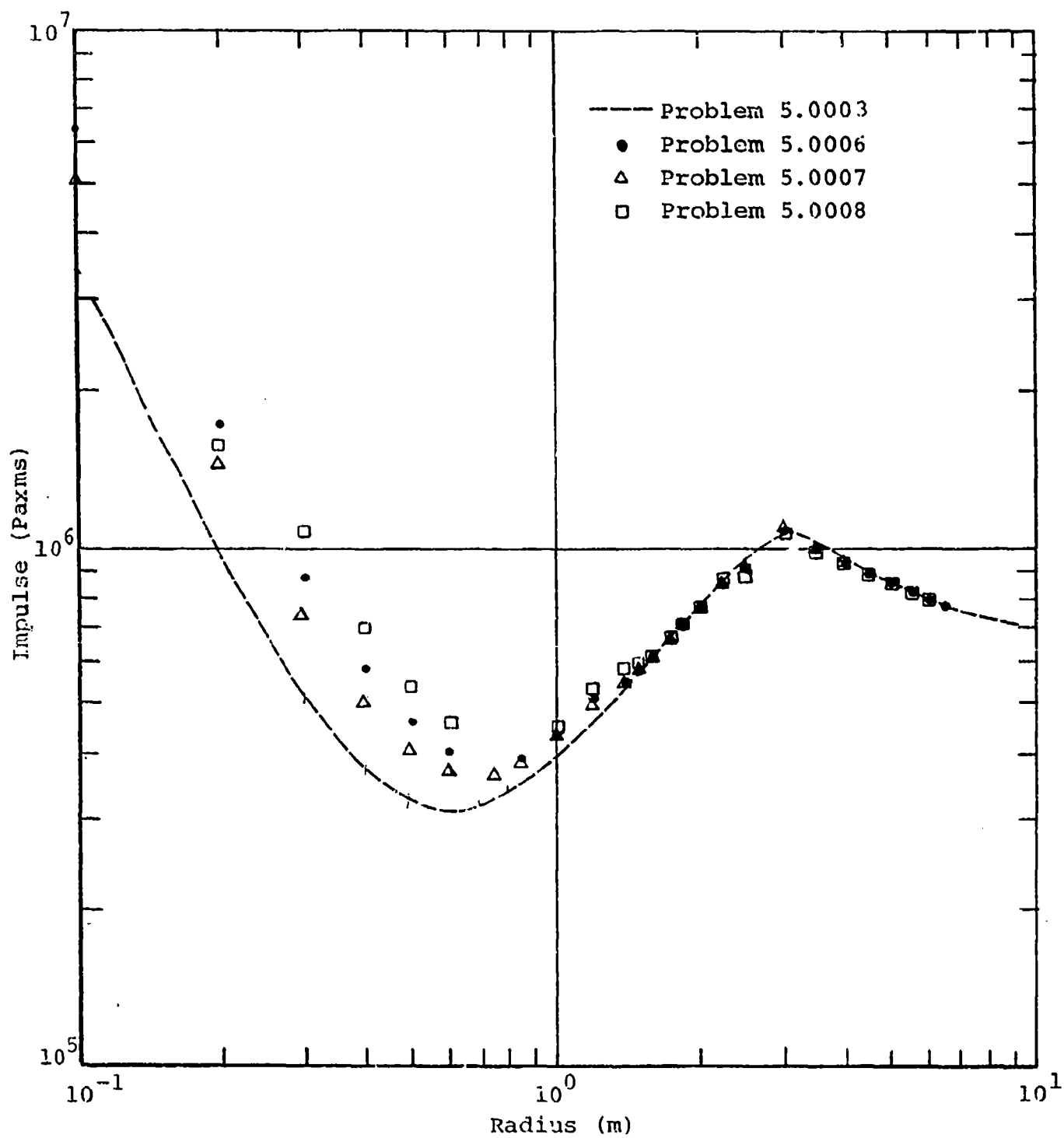
FIGURE 24. Overpressure versus Radius

FIGURE 25.   Overpressure Impulse versus Radius

42

in overpressure impulse, as large as a factor of two, inside
the 2-m radius. Once again, the hollow charge data mimics the
solid charge data after the reflected shock catches the main
shock. The positive phase duration comparisons in Figure 26
show a significant increase in duration for hollow charges.
A factor of 2.5 increase is seen at the 1 m radius from Problem
5.0009.

34. The hollow charge has certain airblast characteristics
of its own. The data reveal that the greatest impulse enhance-
ment occurs in Problem 5.0008, from the charge with a center
volume of twice the charge volume. This would seem to indicate
that the larger the center volume, the greater the increase in
impulse. There is, however, a drawback to this reasoning (aside
from the problems of constructing a charge of this configuration).

35. As the main and reflected shocks separate, a decrease
in overpressure begins to develop between the two shocks
(Figure 27). The overpressure goes negative for some time
before the reflected shock passes through this region. The
result is a pressure-time waveform as shown in Figure 28. The
depth and duration of the first negative phase increases as
the center volume of the charge increases. A trade-off point
exists, therefore, where this brief negative phase negates the
added impulse due to increase in the center volume.

Detonation Treatment Effect on Hollow Charges

36. Problem 5.0009, with isothermal initial conditions,
was run to determine the effect of detonation treatment on the
hollow charge and as a basis of comparison for Problems 5.0010
and 5.0011. Figures 29 through 31 compare the results of
Problems 5.0006 and 5.0009.

37. The results are similar to those for the solid charge
detonation comparisons. Initial pressures for the isothermal
detonation are lower than those for the burn calculation, but
are higher at distances beyond 1 m. The impulse for the
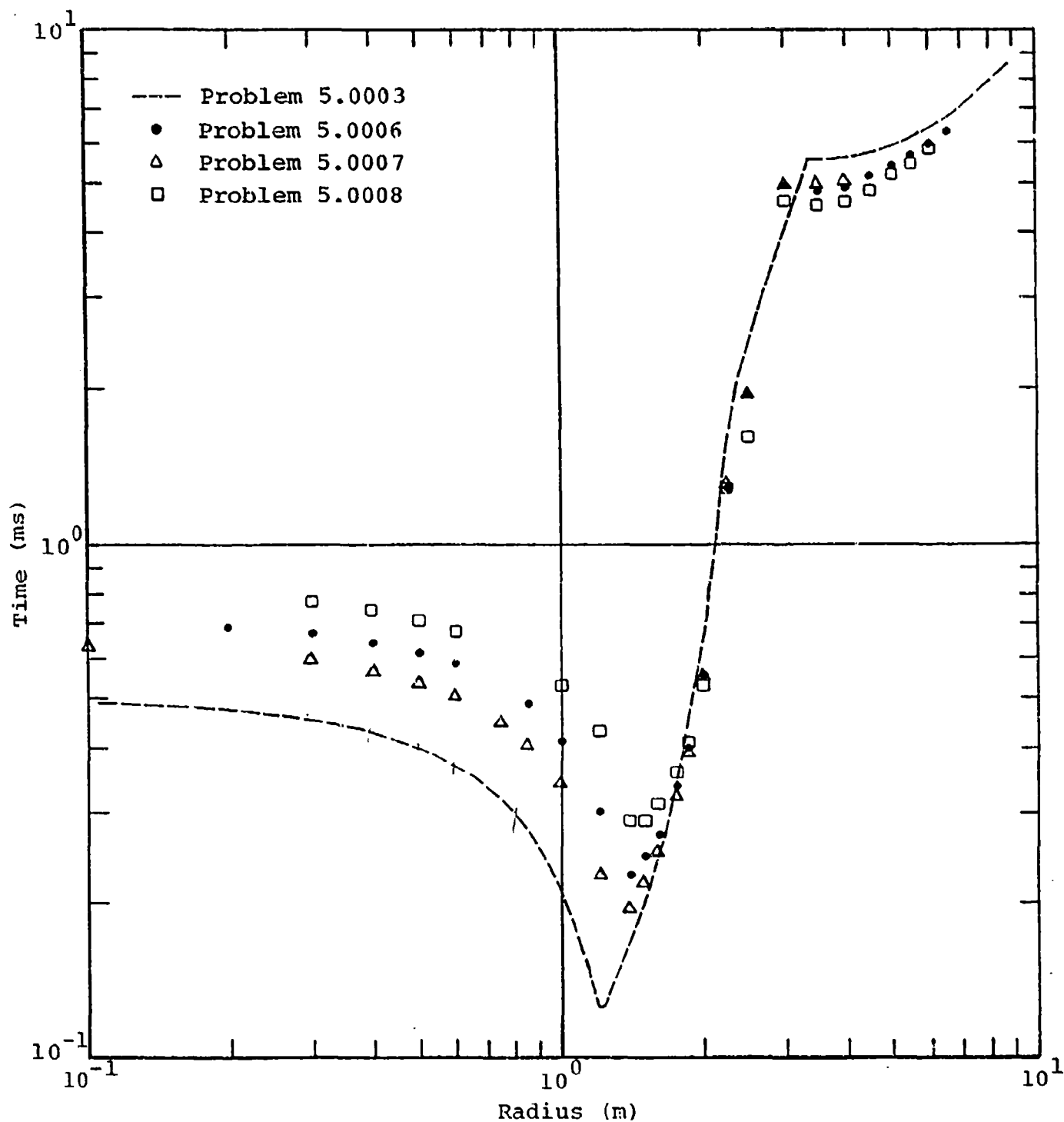
43

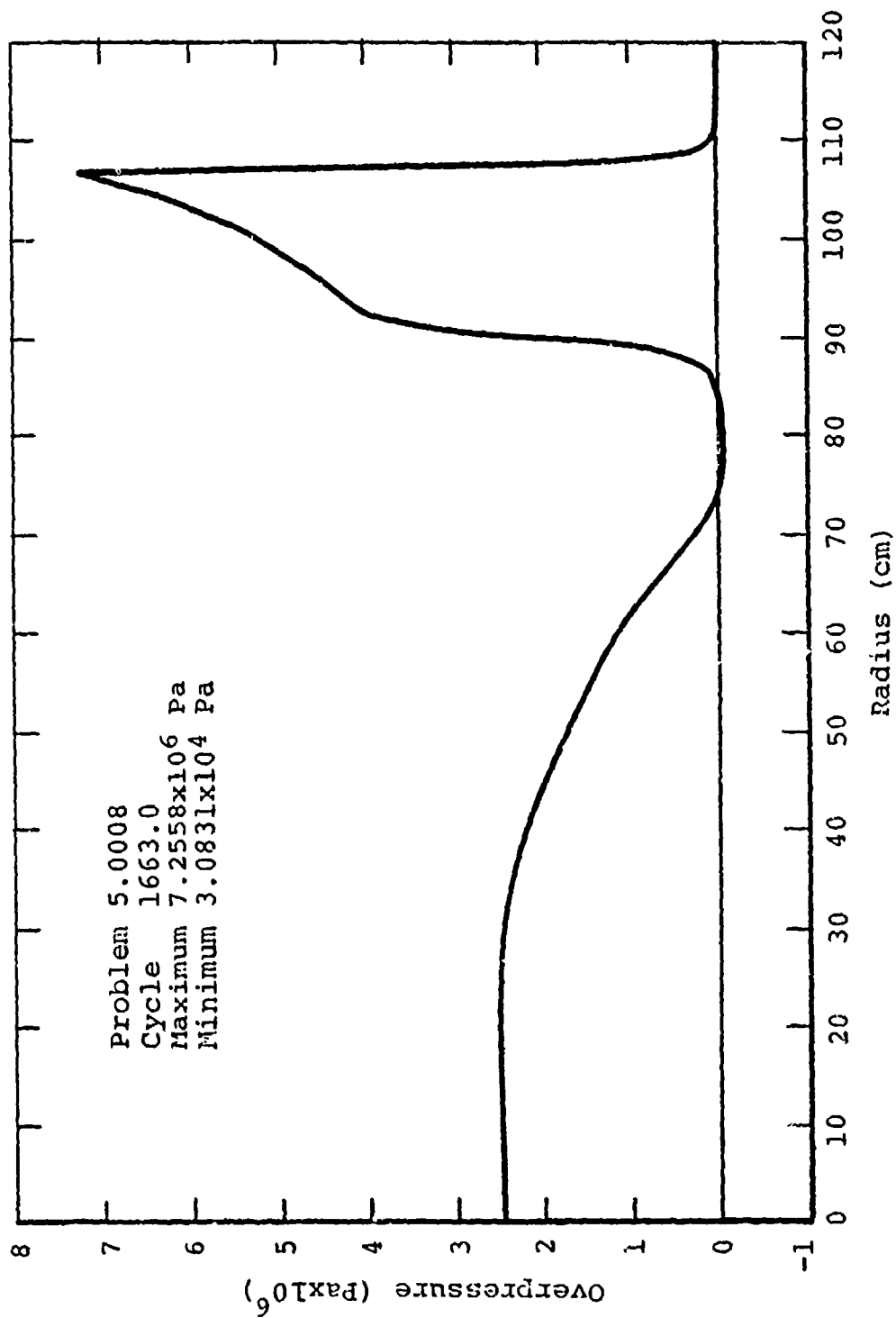FIGURE 26. Positive Phase Duration versus Radius

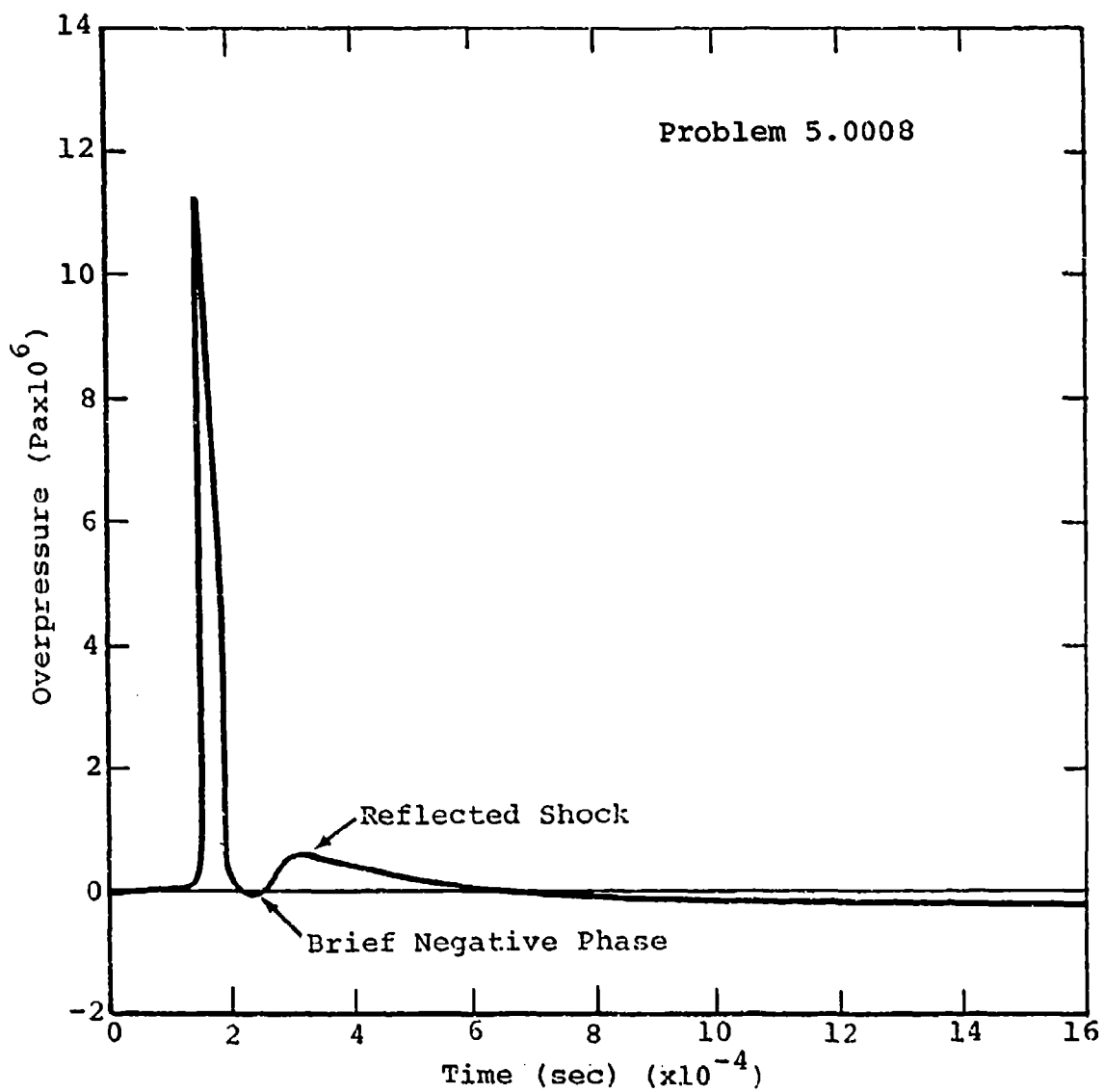FIGURE 27. Overpressure versus Radius at 0.25 msec

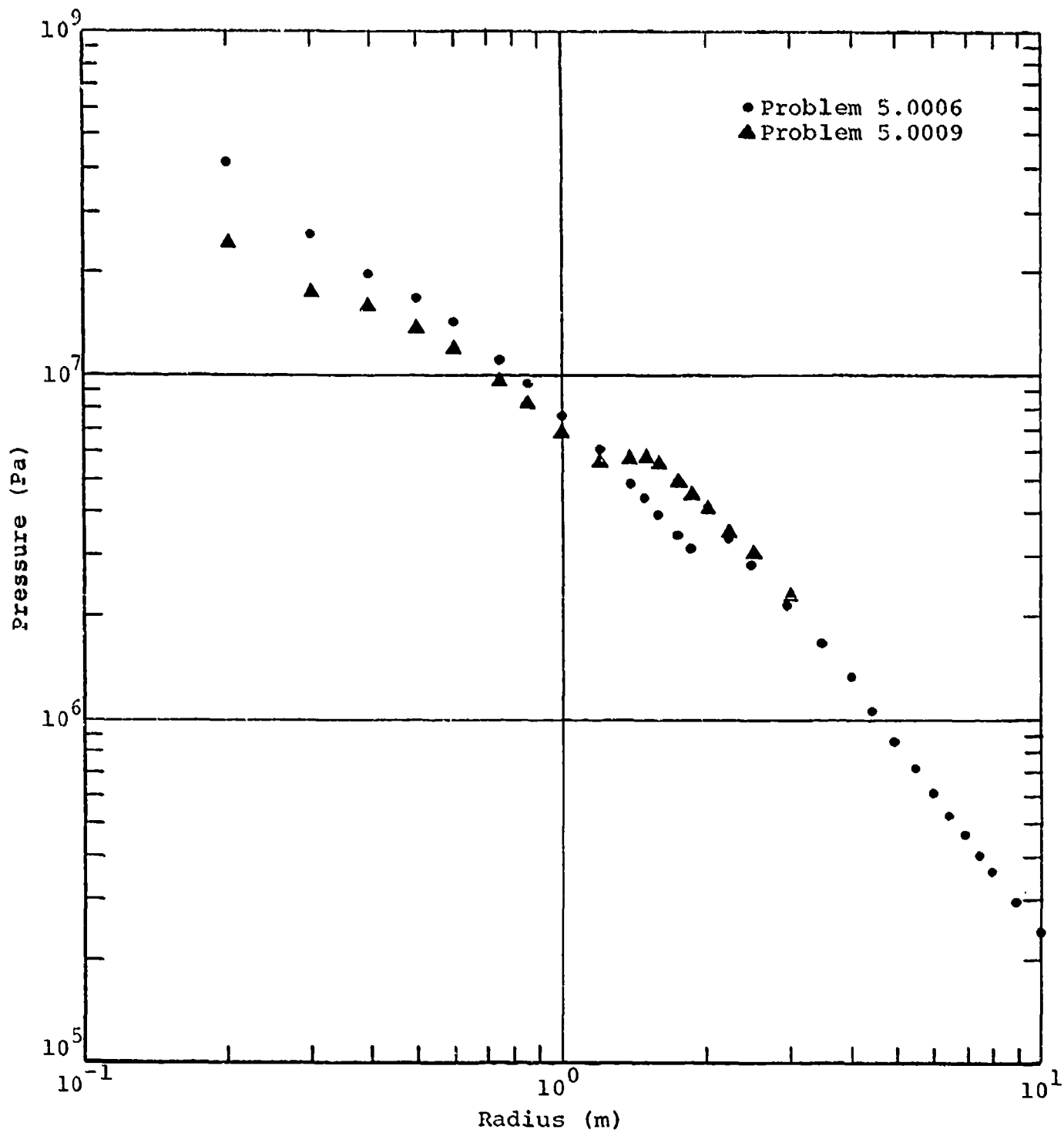FIGURE 28.   Overpressure versus Time at 0.75-m Radius
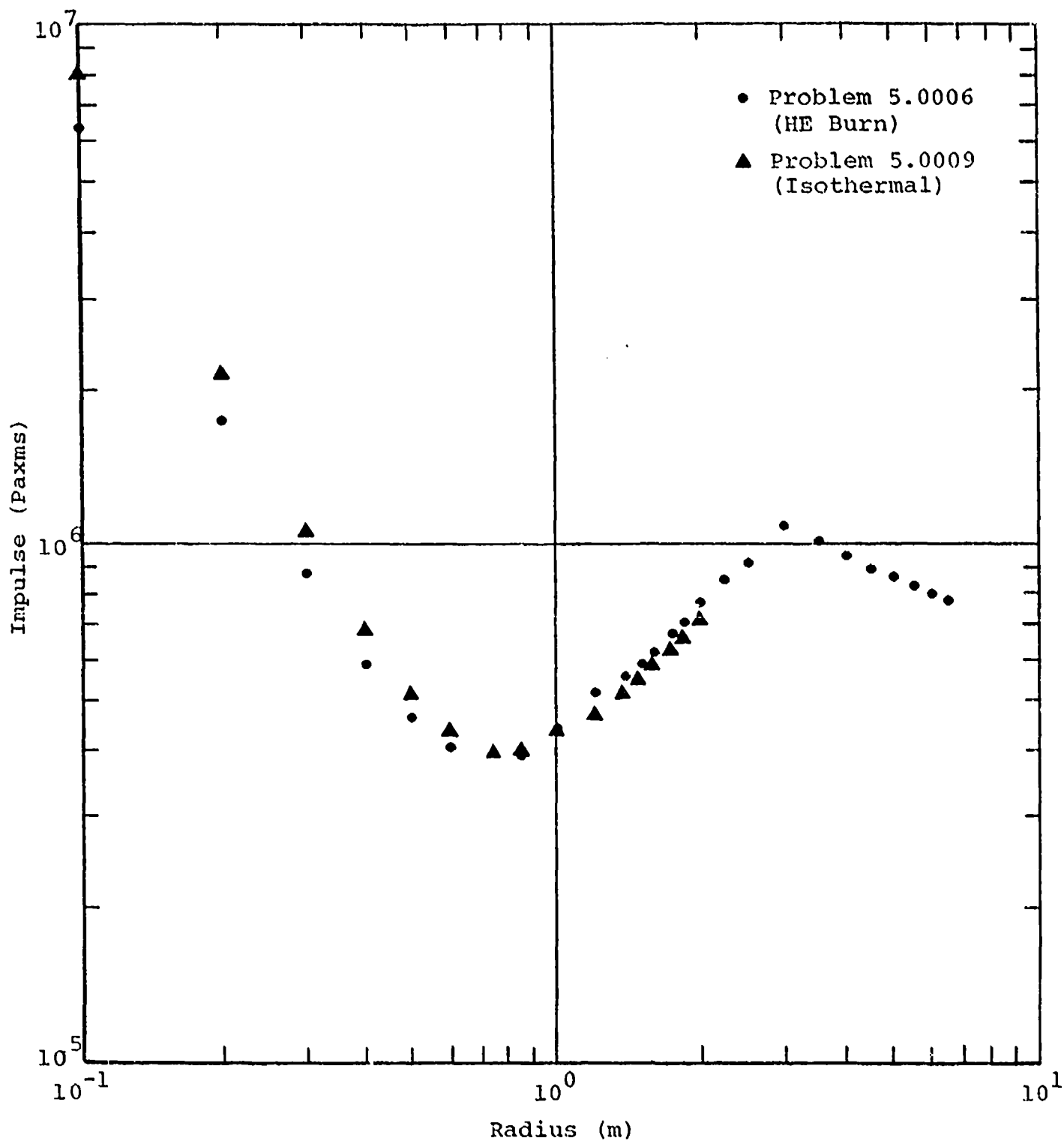
46

FIGURE 29. Peak Overpressure versus Radius

FIGURE 30.   Overpressure Impulse versus Radius, Comparing
Detcnation Methods for Hollow Charge Problems

48

FIGURE 31.   Positive Phase Duration versus Radius

49

isothermal calculation lies above that of the burn calculation inside 1 m, in spite of the fact that the positive phase duration shows very little enhancement. This is due to differences in the overpressure waveform shape in this region.

38. Because an isothermal detonation lacks the initial kinetic energy of an HE burn, larger amounts of energy remain in the center of the charge for a longer time, causing pressures to remain at a high level for a longer time and adding to the impulse. The impulse from the isothermal calculation yields to the higher impulse from the burn at about 1 m. Data from both calculations shoul' come together at greater radii.

Hollow-Charge Variations

39. Based on the results of Problems 5.0006 through 5.0009, two additional hollow-charge calculations were made. Previous hollow-charge calculations revealed that a region of inert material (air) placed in the charge center yielded a significant increase in overpressure impulse in the skip zone. It was noted that an increase in the volume resulted in a proportional increase in impulse. The success of the hollow charge led to an expansion of the principle in the next two calculations.

40. Because of the premature negative phase which was noted in Problem 5.0008, due to the large center volume, we placed a denser material in a smaller center region in Problems 5.0010 and 5.0011. The predicted effect was a slowing of the inward moving shock resulting from the expansion of the detonation products. Impulse enhancement without the effects of a premature negative phase was the desired result.

41. A preliminary attempt to incorporate an equation of state for polystyrene and polyurethane foams[3,4] into the SAP code failed. Incompatabilities with the hydrocode were contributing factors to the inability of the equations of state to perform properly in the region of interest. A suitable equation of state for water, however, was readily available and adapted for use in SAP.

42. Problem 5.0010 calculated hollow-center line charge effects using water in the center volume. A high density, low energy air medium (ρ_o = 100 kg/m^3, E = 2.43x10^{10} ergs/kg) was used in place of foam in Problem 5.0011. The center volumes for both calculations were made equal to the charge volume. As a means of reference, airblast parameters from both calculations are compared with Problems 5.0002 (the solid charge) and 5.0009 (the hollow-center charge) in Figures 32, 33, and 34.

43. In Figure 32, the overpressure profile of Problem 5.0010 follows along Problem 5.0009 to 1.2 m before dropping to a lower pressure level. The jump in pressure seen in Problem 5.0009 is not as pronounced in the water center calculation, meaning that the reflected shock has been weakened somewhat. This weakening is attributed to the large amounts of energy lost in converting the water to steam.

44. This loss of energy is apparent in impulse and positive phase duration comparisons in Figures 33 and 34. Impulse from Problem 5.0010 lies between the solid charge and the hollow-center charge out to a radius of 0.75 m. At this point the water-center calculation intercepts and even falls below the solid charge data. Duration comparisons show only a slight enhancement above the solid charge data between 0.6 and 1.5 m.

45. Overall results of Problem 5.0010 show some enhancement in impulse due to the hollow-charge configuration. The use of water in the center region, however, does not produce the desired effect when compared to a standard hollow charge.

46. What is the effect of a less dense material on the hollow-charge airblast? Problem 5.0011 answers this question by revealing little to no effect, at least for a material 100 times denser than ambient air. In this calculation, air properties were used to simulate a polyurethane air mixture (foam) in the charge center. Air occupied the center region
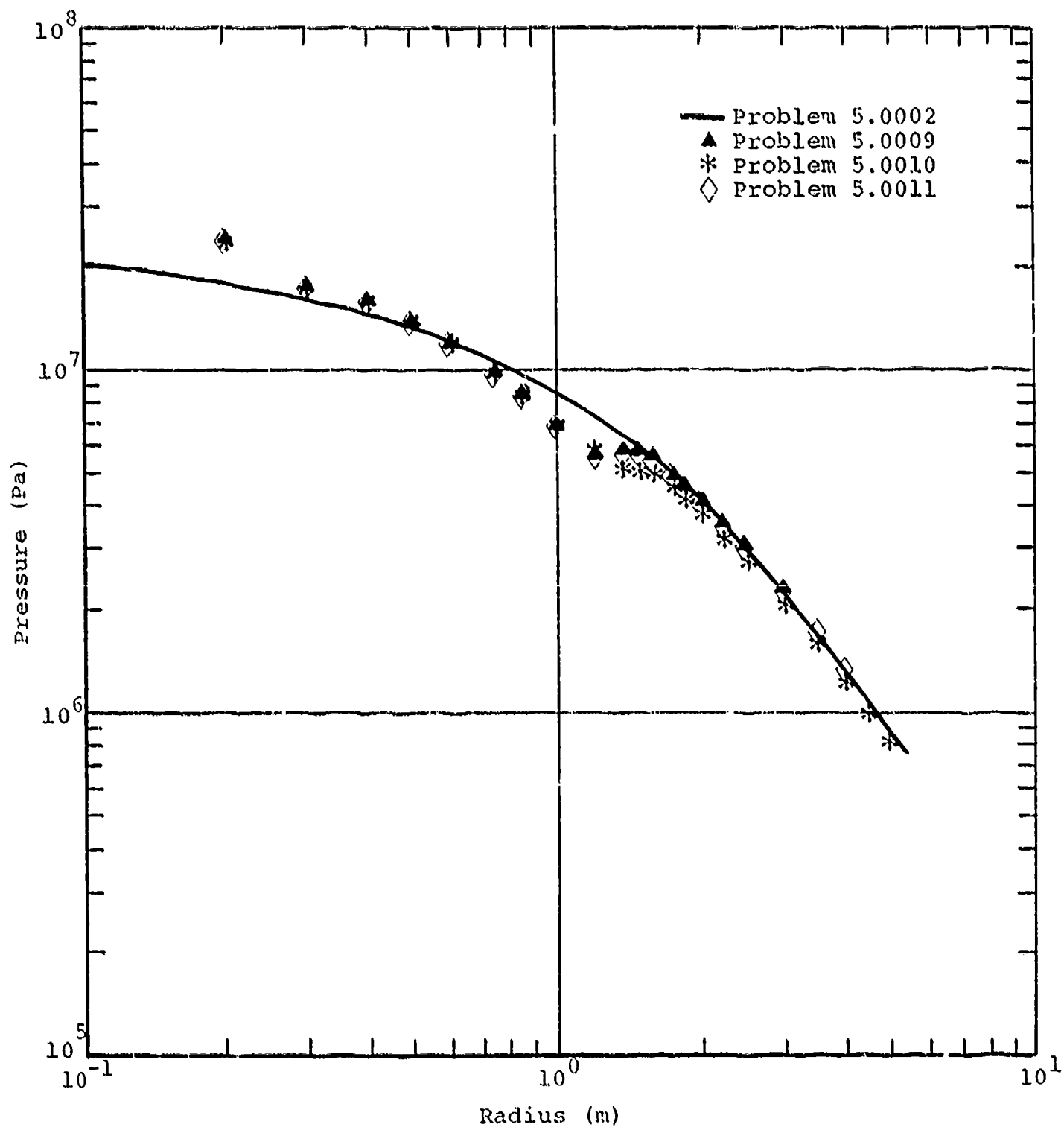
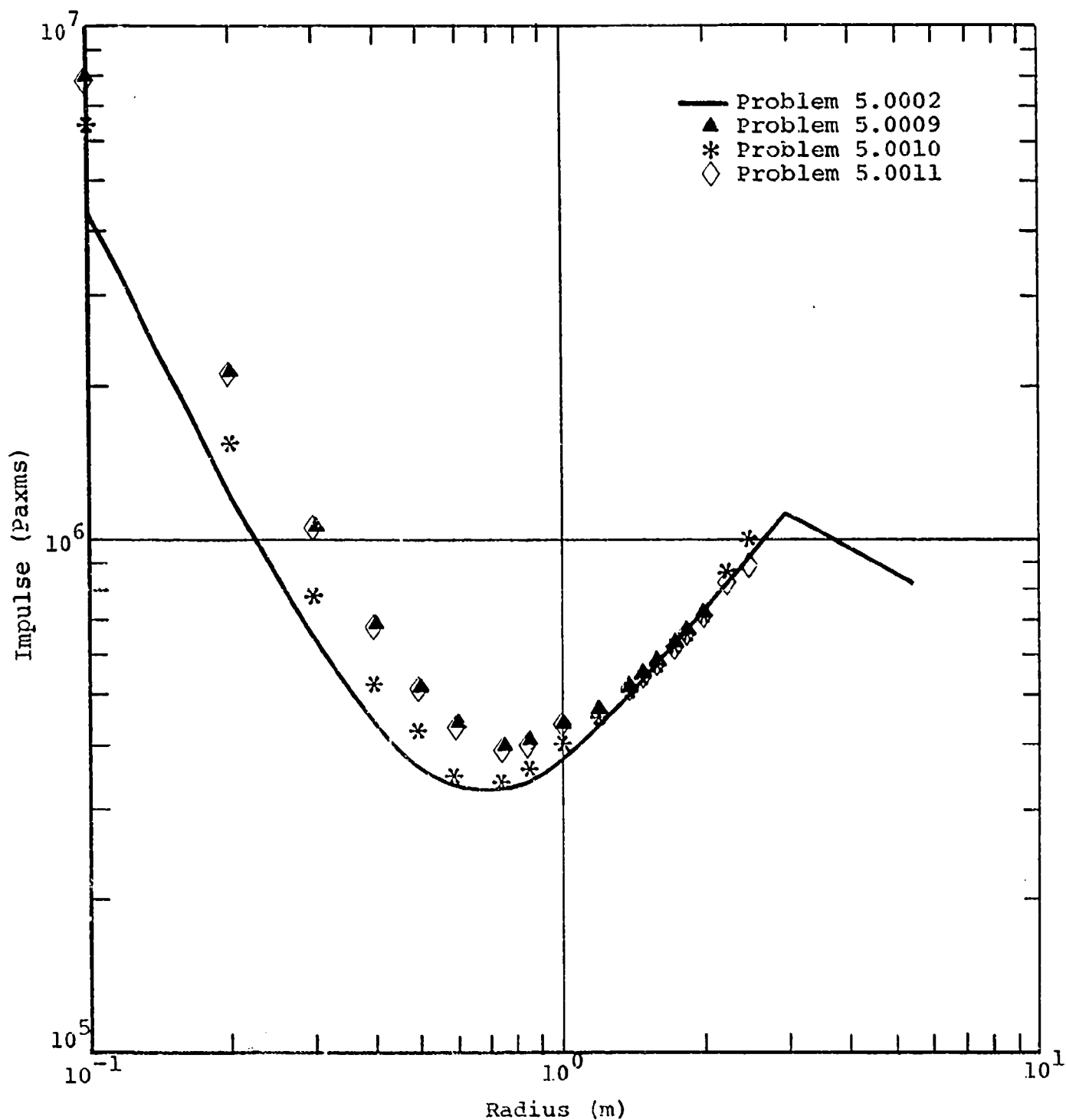FIGURE 32.   Peak Overpressure versus Radius
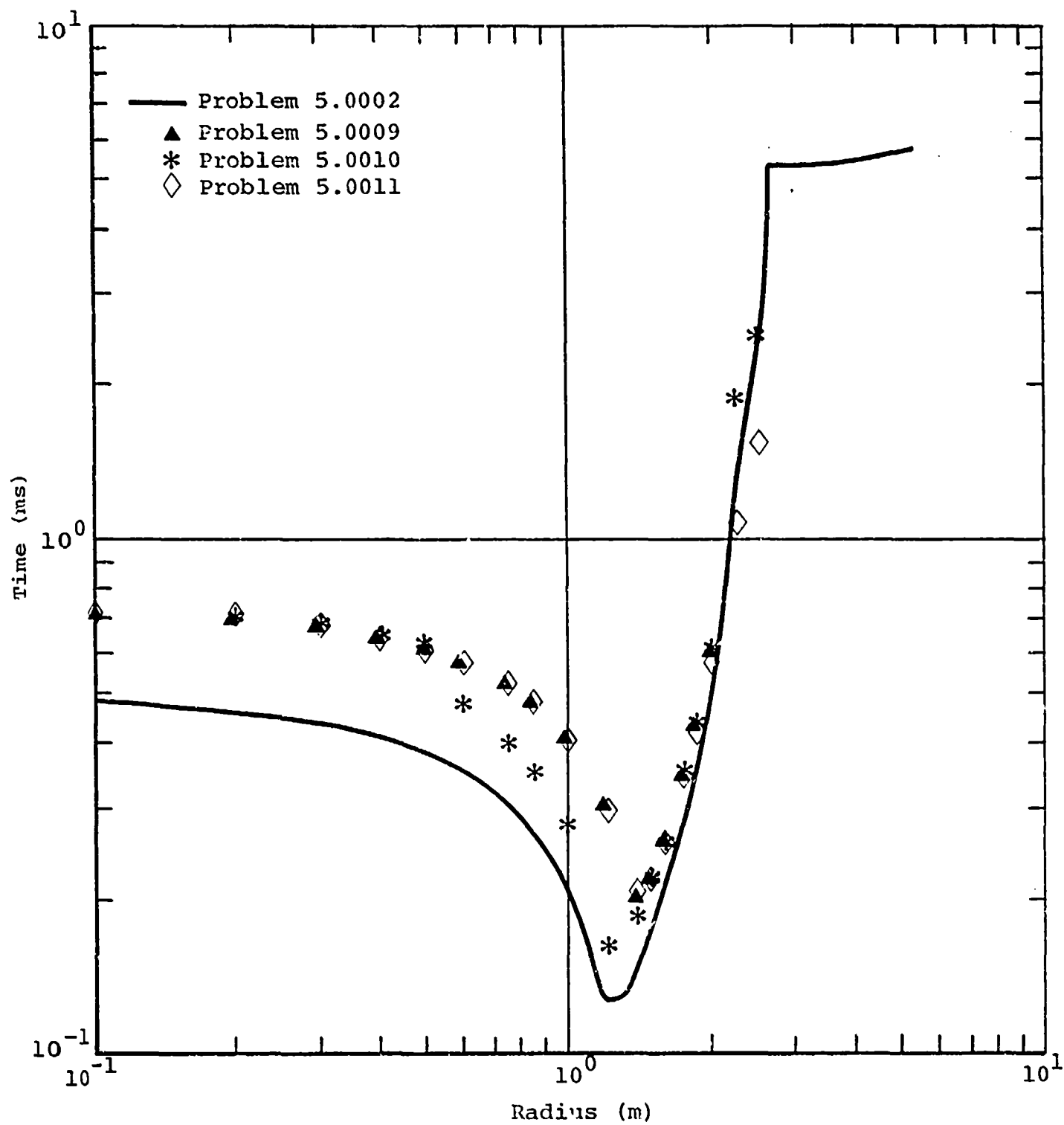
FIGURE 33.   Impulse versus Radius

53

FIGURE 34. Positive Phase Duration versus Radius

54

at a density of 100 kg/m^3. In order to obtain ambient air pressure, the energy of the air was significantly reduced. Comparisons with the hollow-charge calculation (Problem 5.0009) in Figures 32 through 34 show no effect on any of the airblast parameters.

Additional Calculations

47. Two final line-charge improvement calculations were made. Problem 5.0012 is a solid line-charge calculation with a layer of dense material (air) around its outer surface. The purpose of this calculation was to determine the effect of a layer of inert material surrounding the charge. Problem 5.0013 is a variation of the hollow-center calculations. This calculation employed the charge configuration shown in Figure 17, PART III. The main purpose of this calculation was to determine if an even greater impulse enhancement could be achieved through complex shock interactions which take place in the void region between the two HE regions.

48. Problem 5.0012 consisted of a 15.12 kg/m solid line-charge surrounded by a 2-cm layer of dense, low energy air of properties identical to those in Problem 5.0011. The detonation was treated as an isothermal detonation, therefore its impulse profile is compared to those of Problems 5.0002 and 5.0009 in Figure 35. Unlike Problem 5.0011, the presence of the dense material in this exterior region afforded a small increase in impulse to 1.5 m. Enhancement was not as great as that achieved in Problem 5.0009, however.

49. The double-charge calculation (Problem 5.0013) was the final line-charge improvement calculation. Half the total charge mass was placed in each HE region. The purpose of the double-charge configuration was to stretch the region containing detonation products and to generate multiple shock interactions in this region. The results of such interactions were too complex to predict without the hydrocode calculation.
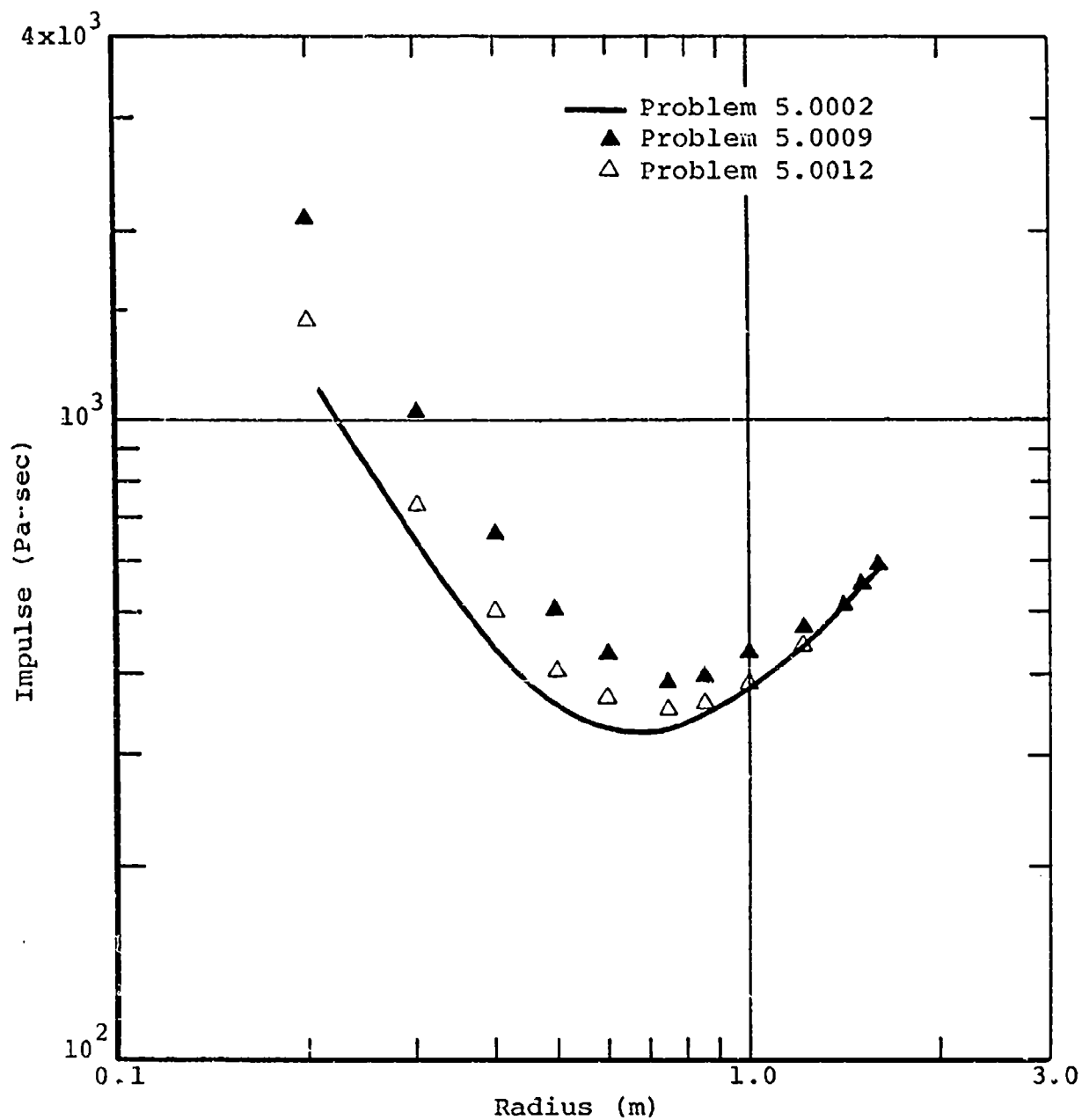
FIGURE 35. Overpressure Impulse versus Radius

56

50. Figures 36 through 38 compare airblast parameters from Problem 5.0013 with those from Problem 5.0009. A few subtle differences occur between the two calculations. Positive phase overpressure comparisons reveal that double charge pressures are lower out to 0.5 m. Inward and outward-moving shocks from both HE regions are generated during the detonation. The shocks reflect from each other in the region of air between the two HE regions at early times. The reflected inward moving shock catches up to the main shock at about 0.6 m, as indicated by the rise in peak pressure in Figure 36. An almost undetectable rise in pressure occurs again at just over 2 m, marking the point where the second shock has caught the main shock after reflecting from the charge center.

51. The secondary shock interactions from the double charge have very little effect on hollow-charge impulse, as is evident in Figure 37. The impulse profile from the double charge lies on top of the hollow-charge data of Problem 5.0009. Overpressure positive phase duration also shows only a slight difference, except in the region 1.2 to 2 m, as demonstrated in Figure 38.

52. Close analysis of the double-charge calculation does reveal one important point. The inward moving shock of the outer HE region overwhelms the outward moving shock of the inner HE region when they reflect from each other. The reason is that the inward moving shock gains strength due to cylindrical convergence as it moves inward. When the shocks reflect, the outward moving shock is weakened significantly. In order to strengthen this shock, logic suggests a reduction in the charge mass in the outer HE region. This would also tend to increase impulse at small radii. A trade-off point exists where the proper ratio of inner-to-outer region charge mass will yield maximum impulse enhancement.
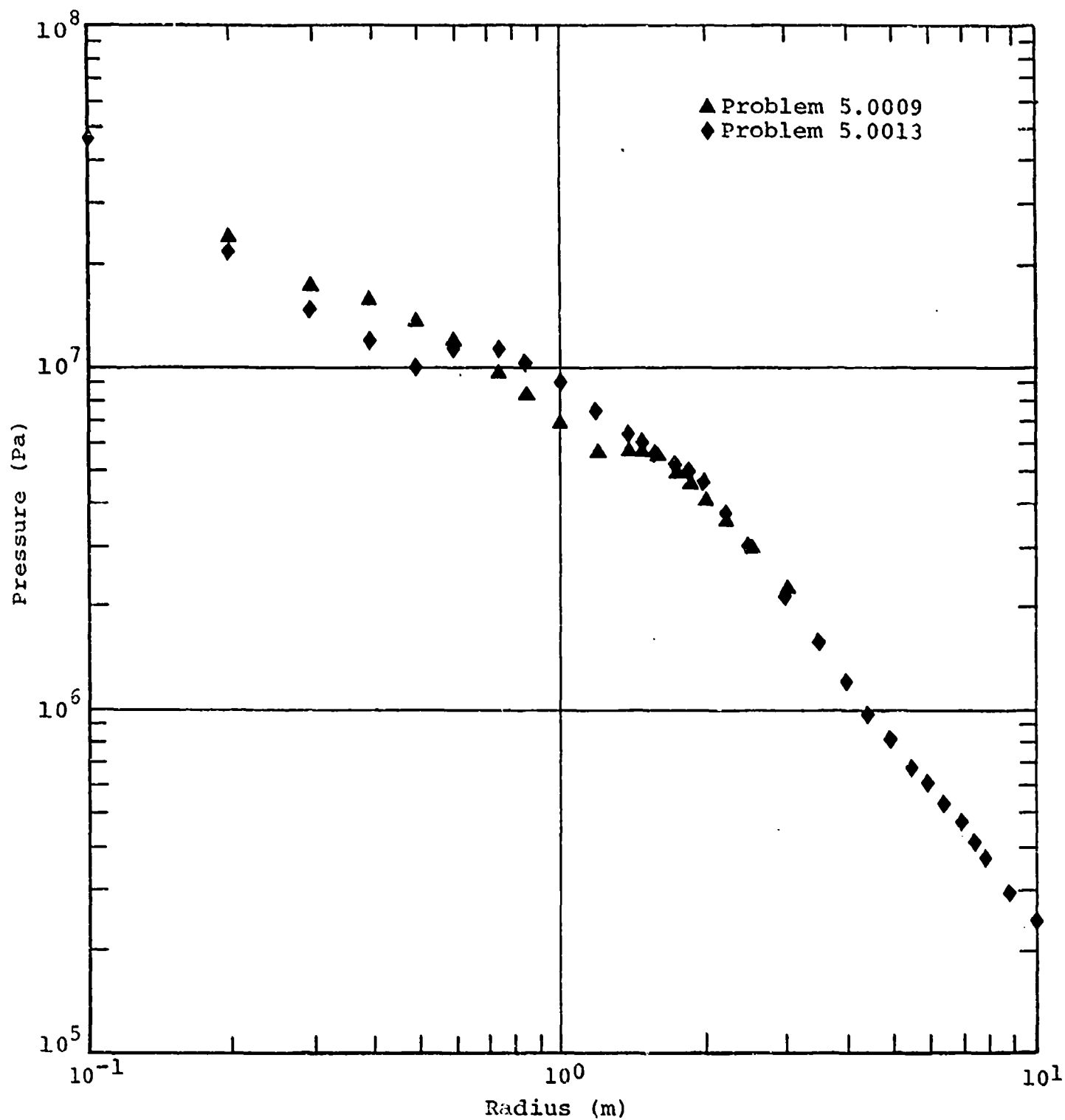
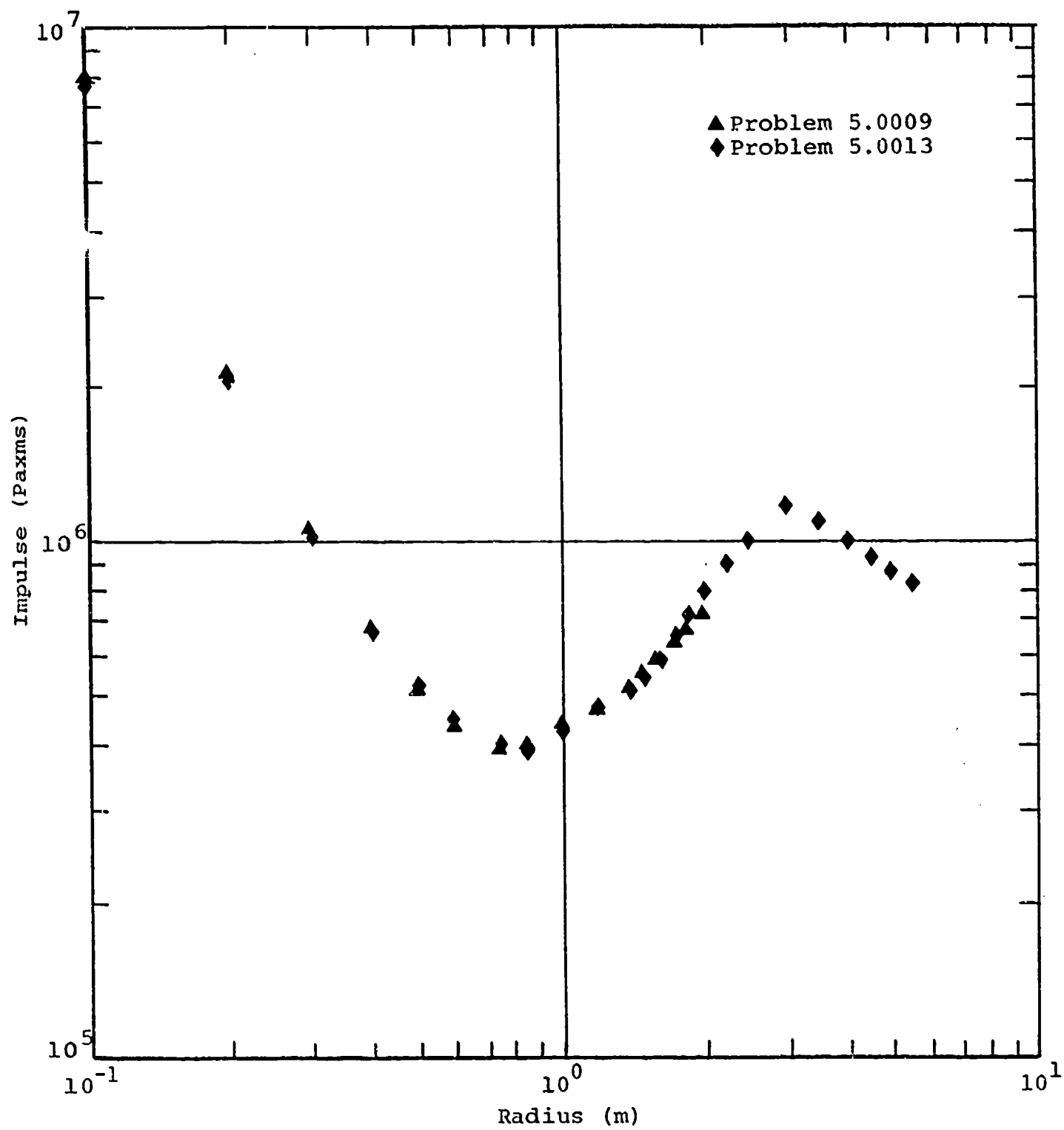FIGURE 36. Peak Overpressure versus Radius
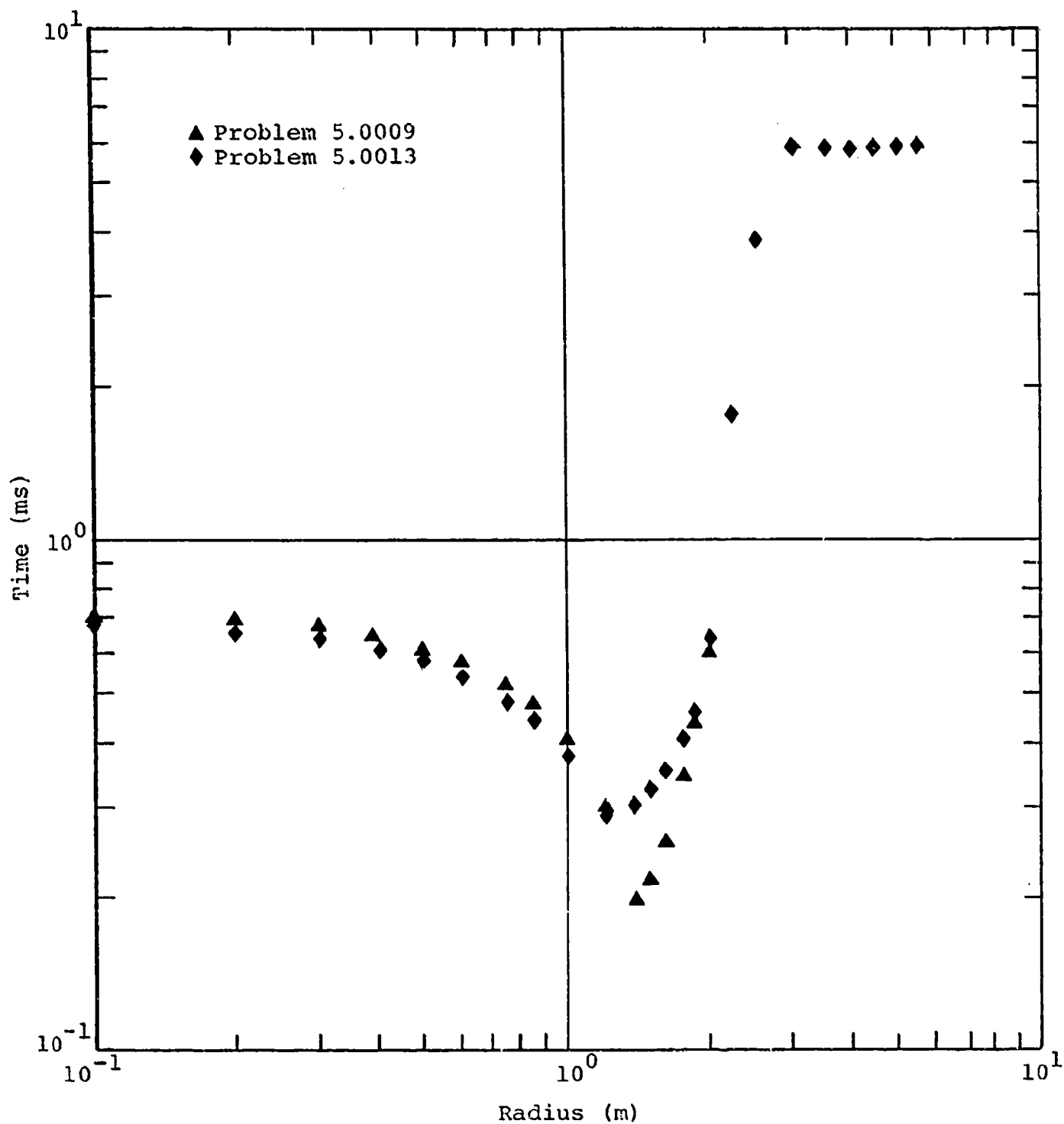
FIGURE 37.   Impulse versus Radius

FIGURE 38. Positive Phase Duration versus Radius

PART V. LINE-CHARGE IMPROVEMENT TESTS

53. Based on preliminary results of the hollow-charge calculations, a series of tests was conducted by WES to determine the validity of the calculations. Overpressure gage recordings were made at several radii. Only one recording in the skip zone was made because gages were not available to record the high pressures in this region. Three gages were damaged or lost in attempts to make high-pressure measurements. A complete set of recordings was sent to S^3 for comparison and evaluation[5].

Charge Design and Experimental Procedure

54. The test series consisted of a total of six events. Two of the events were solid-charge control shots consisting of line charges at a density of 5.74 kg/m. Two events were hollow line-charges consisting of a 3-inch pipe inside a 4-inch pipe with explosive in the space between the pipes. The charge density was 2.57 kg/m. Two events used a 2-inch inside a 4-inch pipe and had a charge density of 6.6 kg/m.

55. Hollow-charge containers were constructed of commercially available PVC pipe approximately 6 m in length. The smaller pipe was centered inside the larger pipe and nitromethane was poured into the space between the two pipes. Because of difficulties in sustaining detonation in a hollow charge, a commercially available sensitizer was mixed with the nitromethane to ensure full detonation.

Experimental Results

56. Using experimental gage recordings, peak overpressure and overpressure impulse data were tabulated from two of the hollow-charge events and one of the solid-charge events (see Appendix A). These events are referred to as LCI-II-1, LCI-II-2, and LCI-II-5, respectively. Results of calculations

61

(Problems 5.0003, 5.0006, and 5.0008) are used for comparison purposes. Because the yields of the experiments and calculations were not the same, the data presented were scaled to the yield of LCI-II-1 and LCI-II-2 (2.57 kg/m). Square root scaling to the charge density ratios was used. Experimental data from LCI-II-1 and LCI-II-2 were averaged and error bands were placed on the data.

57. Figure 39 is a comparison of overpressure from LCI-II-1 and LCI-II-2 with Problems 5.0006 and 5.0008. The experiments used a void fraction (ratio of center volume to charge volume) of approximately 1.28. Problem 5.0006 had a void fraction of one and Problem 5.0008 had a void fraction of two. The calculational data falls near the data scatter out to a radius of 2.5 m and shows excellent overall agreement in peak pressures. At about 1.1 m, the pressure from Problem 5.0006 rises, marking the merging of the main and reflected shocks. The merging occurs at 1.3 m in Problem 5.0008. The experimental data between 1.1 and 1.4 m also shows a similar rise. The rise in the experimental data occurs between the two calculations as would be expected from the volume ratios.

58. The merging of the second shock with the main shock is an important parameter for these experiments. The second shock has passed through the interior of the charge and has been changed by the conditions existing in the skip zone. The fact that the calculations agree with the radius of merging and with the peak overpressure in this vicinity is a strong indication that the blast parameters are properly treated by the calculations in the range less than 1 m.

59. Impulse comparisons are given in Figure 40. These also reveal excellent agreement between calculation and experiment. The impulse minimum is not shown by the experiments because gage recordings were only made as close as 0.81 m. The calculation is again within data scatter out to 3 m and is slightly above the experimental data beyond 3 m.
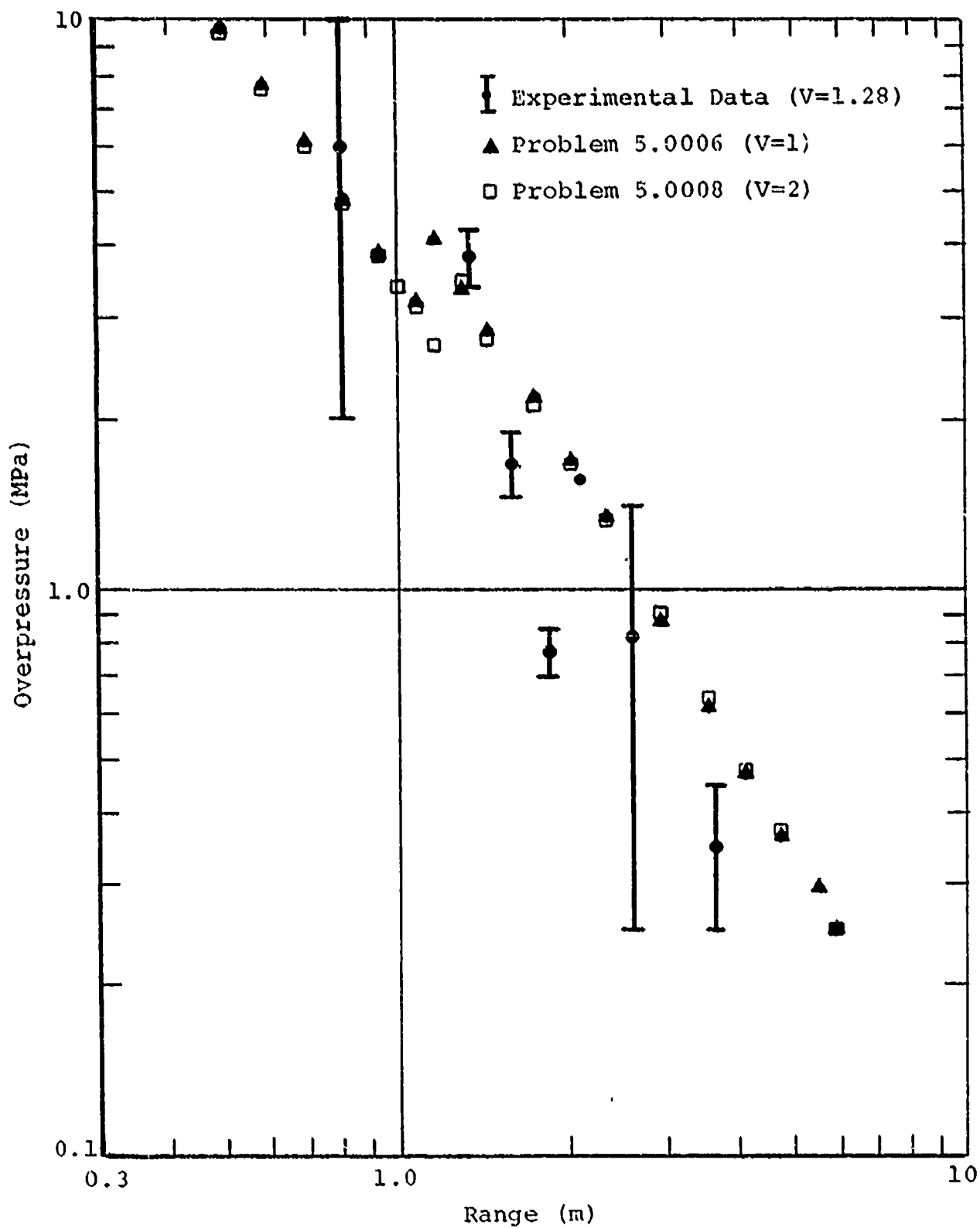
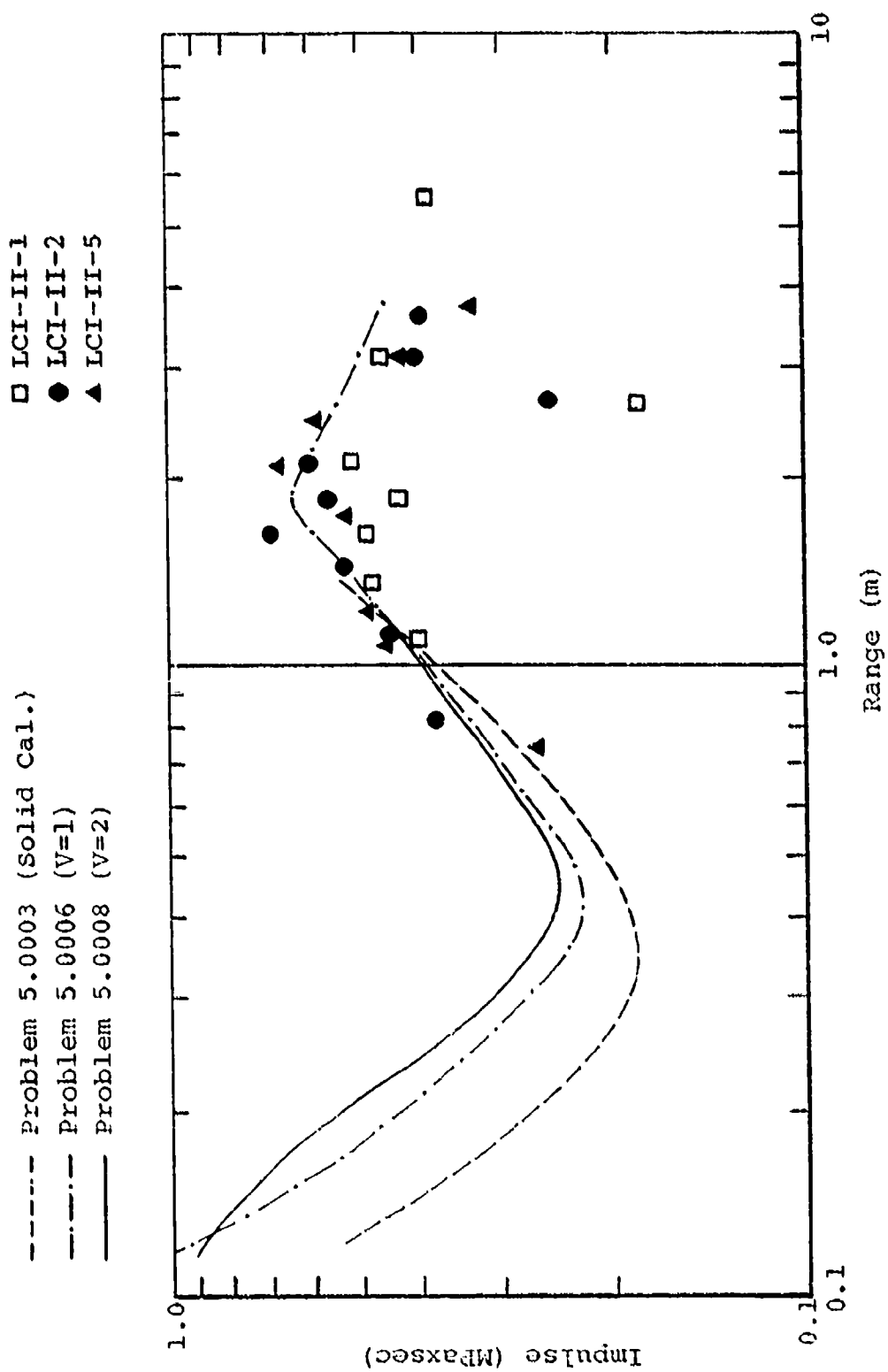FIGURE 39. Overpressure versus Radius, Hollow Charges

FIGURE 40. Impulse

60. Data from LCI-II-5 is compared to Problem 5.0003 in Figure 40 and to earlier solid charge experiments (LCI-II-6, LCI-2, and LCI-3) and Problem 5.0003 in Figure 41. Figure 41 shows agreement of experimental solid charge overpressures and calculations. Impulse comparisons in Figure 40 reveal remarkable similarities with calculational impulse data. Experimental hollow charge data lie above the solid charge data inside 1 m, implying impulse enhancement in this region.

61. The question arises as to whether the experimental solid charge data inside 1 m is reliable. This can be shown by a comparison with impulse data from Problem 5.0003 in Figure 40. Because calculational and experimental solid charge data are in excellent agreement, one may conclude that the experimental data points are valid.

62. In reference to the comparisons, several important points can be made:

a. Hollow-charge data from experiment and calculation are in good overall agreement.

b. Hollow-charge characteristics predicted by the calculations are evident in experimental data.

c. Solid-charge experimental and calculational data show excellent agreement.

d. Overpressure impulse enhancement in the skip zone for hollow charges is seen in experimental data as predicted by the calculations.

63. As reported in Reference 5, an effort is underway to determine if the achieved enhancement is sufficient to reliably activate the M16 AT mine.
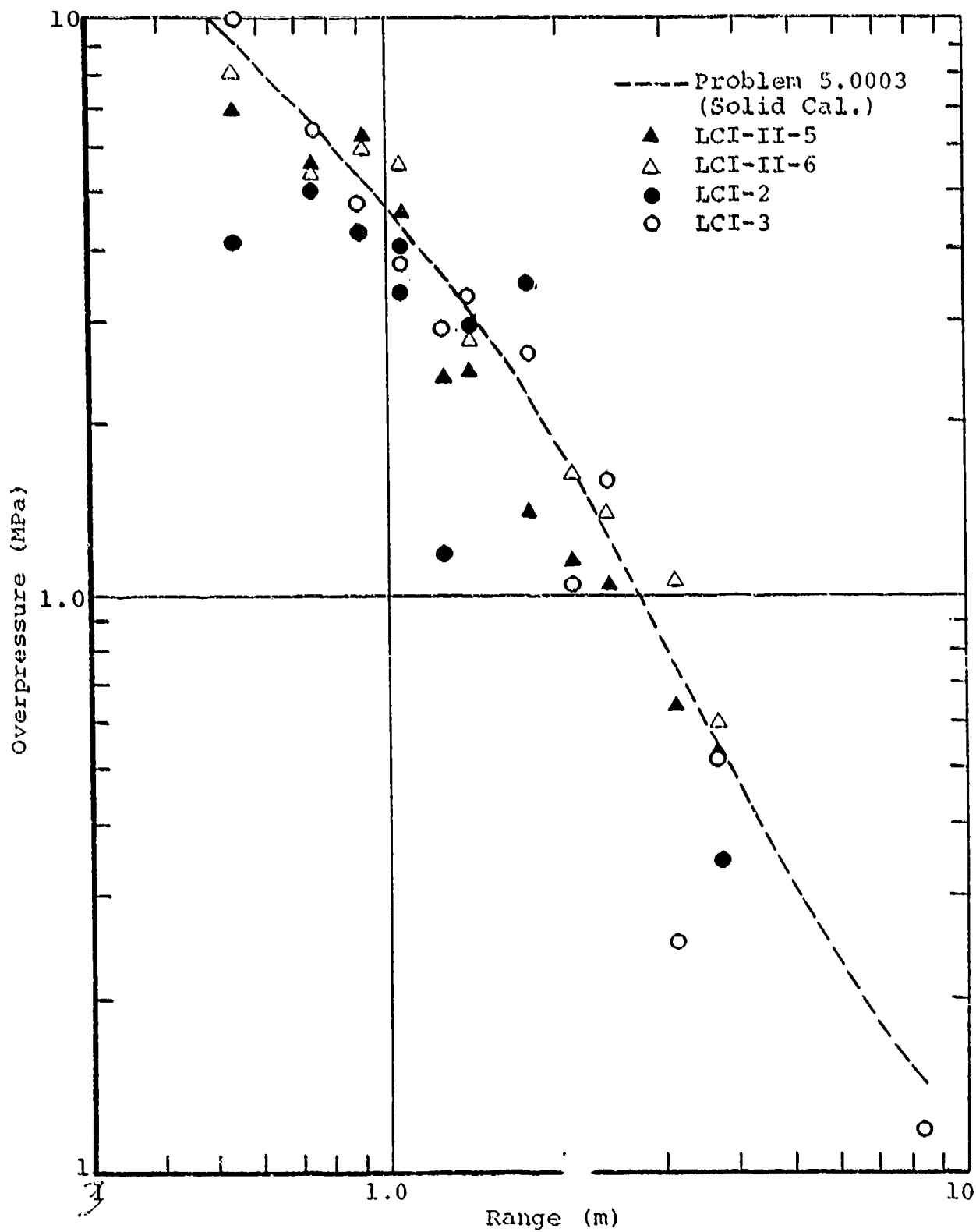
FIGURE 41.   Overpressure versus Radius, Solid Charges

66

References

1. Ingram, J. K., "Airblast and Impulse Produced by M58 Al and British Giant Viper Linear Explosive Charges - Phase 2 Experiments", Preliminary Report, November 1979, U.S. Army Engineer Waterways Experiment Station, Vicksburg, Mississippi.

2. Whitaker, W. A., et.al., "Theoretical Calculations of the Phenomenology of HE Detonations", AFWL-TR-66-141, Volume I, November 1966, Air Force Weapons Laboratory, Research and Technology Division, Kirtland Air Force Base, New Mexico.

3. Ree, Francis H., "Equation of State of Plastics: Polystyrene and its Foams", UCRL-51885, August 1975, Lawrence Livermore Laboratory, University of California, Livermore, California 94550.

4. Mader, C. L., Carter, W. J., "An Equation of State for Shocked Polyurethane Foam", LA-4059, UC 34, Physics, TID-4500, Written: November 1968 Distributed: February 1969, Los Alamos Scientific Laboratory of the University of California, Los Alamos, New Mexico.

5. Ford, M. B., "Line-Charge Improvement Tests", WEESE, Unpublished Working Draft, July 1981, U.S. Army Engineer Waterways Experiment Station, Vicksburg, Mississippi.

APPENDIX A

Tabulated Data from Gage Records

1. EVENT LCI-II-1

Radius (m)	Overpressure (MPa)	Overpressure Impulse (kPa-sec)
0.81	10+	0.41
1.1	2.15	0.475
1.36	4.3	0.48
1.61	1.45	0.43
1.86	0.70	0.51
2.11	1.6	0.18
2.61	0.25	0.45
3.11	0.375	0.4
3.61	0.25	0.39
5.5	0.3	

2. EVENT LCI-II-2

Radius (m)	Overpressure (MPa)	Overpressure Impulse (kPa-sec)
0.81	2+	0.38
1.1	2.4	0.44
1.36	3.4	0.515
1.61	1.9	0.69
1.86	0.85	0.56
2.11	1.5	0.59
2.61	1.4	0.255
3.11	0.4	0.41
3.61	0.45	0.4

Tabulated Data from Gage Records (Continued)

3.   EVENT LCI-II-5 (Scaled to a charge density of 2.57 kg/m)

Radius (m) (scaled)	Overpressure (MPa)	Overpressure Impulse (kPa-sec) (scaled)
0.54	7.0	0.228
0.74	5.65	0.265
1.07	4.62	0.44
1.24	2.4	0.479
1.74	1.4	0.53
2.18	1.15	0.67
2.45	1.05	0.585
3.15	0.65	0.425
3.71	0.54	0.33